Scott LJ, McKeage K, Keam SJ, and Plosker GL (2003) Tacrolimus: a further update of its use in the management of organ transplantation. *Drugs* **63:**1247–1297.
Uwai Y, Masuda S, Goto M, Motohashi H, Saito H, Okuda M, Nakamura E, Ito N, Ogawa O, and Inui K (2004) Common single nucleotide polymorphisms of the MDR1 gene have no influence on its mRNA expression level of normal kidney cortex and renal cell carcinoma in Japanese nephrectomized patients. *J Hum Genet* **49:**40–45.
Venkataramanan R, Swaminathan A, Prasad T, Jain A, Zuckerman S, Warty V, McMichael J, Lever J, Burckart G, and Starzl T (1995) Clinical pharmacokinetics of tacrolimus. *Clin Pharmacokinet* **29:**404–430.
Wakasugi H, Yano I, Ito T, Hashida T, Futami T, Nohara R, Sasayama S, and Inui K (1998) Effect of clarithromycin on renal excretion of digoxin: interaction with P-glycoprotein. *Clin Pharmacol Ther* **64:**123–128.
Yasuhara M, Hashida T, Toraguchi M, Hashimoto Y, Kimura M, Inui K, Hori R, Inomata Y, Tanaka K, and Yamaoka Y (1995) Pharmacokinetics and pharmacodynamics of FK 506 in pediatric patients receiving living-related donor liver transplantations. *Transplant Proc* **27:**1108–1110.
Yousem SA, Sartori D, and Sonmez-Alpan E (1993) Multidrug resistance in lung allograft recipients: possible correlation with the development of acute and chronic rejection. *J Heart Lung Transplant* **12:**20–26.
Zahir H, McCaughan G, Gleeson M, Nand RA, and McLachlan AJ (2004) Factors affecting variability in distribution of tacrolimus in liver transplant recipients. *Br J Clin Pharmacol* **57:**298–309.

Address correspondence to: Dr. Ken-ichi Inui, Department of Pharmacy, Kyoto University Hospital, Sakyo-ku, Kyoto 606-8507, Japan. E-mail: inui@kuhp.kyoto-u.ac.jp

Impact of MDR1 and CYP3A5 on the oral clearance of tacrolimus and tacrolimus-related renal dysfunction in adult living-donor liver transplant patients

Masahide Fukudo[a], Ikuko Yano[a], Atsushi Yoshimura[a], Satohiro Masuda[a], Miwa Uesugi[a], Keiko Hosohata[a], Toshiya Katsura[a], Yasuhiro Ogura[b], Fumitaka Oike[b], Yasutsugu Takada[b], Shinji Uemoto[b] and Ken-ichi Inui[a]

Objective **The potential influence of the multidrug resistance 1 (*MDR1*) gene and the cytochrome P450 (CYP) genes, *CYP3A4* and *CYP3A5*, on the oral clearance (CL/F) of tacrolimus in adult living-donor liver transplant patients was examined. Furthermore, the development of renal dysfunction was analyzed in relation to the *CYP3A5* genotype.**

Methods **Sixty *de novo* adult liver transplant patients receiving tacrolimus were enrolled in this study. The effects of various covariates (including intestinal and hepatic mRNA levels of MDR1 and CYP3A4, measured in each tissue taken at the time of transplantation, and the *CYP3A5*3* polymorphism) on CL/F during the first 50 days after surgery were investigated with the nonlinear mixed-effects modeling program.**

Results **CL/F increased linearly until postoperative day 14, and thereafter reached a steady state. The initial CL/F immediately after liver transplantation was significantly affected by the intestinal MDR1 mRNA level ($P<0.005$). Furthermore, patients carrying the *CYP3A5*1* allele in the native intestine, but not in the graft liver, showed a 1.47 times higher (95% confidence interval, 1.17–1.77 times, $P<0.005$) recovery of CL/F with time than patients having the intestinal *CYP3A5*3/*3* genotype. The cumulative incidence of renal dysfunction within 1 year after transplantation, evaluated by the Kaplan–Meier method, was significantly associated with the recipient's but not donor's *CYP3A5* genotype (**1/*1* and **1/*3* vs. **3/*3*: recipient, 17 vs. 46%, $P<0.05$; donor, 35 vs. 38%, $P=0.81$).**

Conclusion **These findings suggest that the *CYP3A5*1* genotype as well as the MDR1 mRNA level in enterocytes contributes to interindividual variation in the CL/F of tacrolimus in adult recipients early after living-donor liver transplantation. Furthermore, CYP3A5 in the kidney may play a protective role in the development of tacrolimus-related nephrotoxicity. *Pharmacogenetics and Genomics* 18:413–423 © 2008 Wolters Kluwer Health | Lippincott Williams & Wilkins.**

Pharmacogenetics and Genomics 2008, 18:413–423

Keywords: CYP3A5, living-donor liver transplantation, multidrug resistance 1, nephrotoxicity, pharmacogenomics, pharmacokinetics, tacrolimus

[a]Department of Pharmacy, Kyoto University Hospital, Faculty of Medicine and [b]Department of Surgery, Graduate School of Medicine, Kyoto University, Kyoto, Japan

Correspondence to Professor Ken-ichi Inui, PhD, Department of Pharmacy, Kyoto University Hospital, Sakyo-ku, Kyoto 606-8507, Japan
Tel: +81 75 751 3577; fax: +81 75 751 4207; e-mail: inui@kuhp.kyoto-u.ac.jp

Received 14 July 2007 **Accepted** 23 January 2008

Introduction

Initially, living-donor liver transplantation (LDLT) was adapted mainly to children with end-stage liver diseases, such as biliary atresia and hepatoblastoma [1]. At present, the technique is used as a treatment option for adult patients with viral hepatic cirrhosis or hepatocellular carcinoma, etc. [2].

Tacrolimus, an immunosuppressant widely used in liver transplantation, has a narrow therapeutic window (5–15 ng/ml) and shows considerable interindividual and intraindividual variability in clinical pharmacokinetics [3,4]. Therefore, therapeutic drug monitoring (TDM) is needed to individualize the tacrolimus dosage for the prevention of allograft rejection as well as adverse effects such as nephrotoxicity [5,6]. Tacrolimus is primarily metabolized by hepatic cytochrome P450 (CYP) 3A4 and 3A5 with the majority of the metabolites eliminated into bile [7]. P-glycoprotein, which is a product of the multidrug resistance 1 (*MDR1/ABCB1*) gene, plays an important role in limiting the oral absorption of immunosuppressive drugs [7]. We clarified that the intestinal MDR1 mRNA affects the postoperative trough levels of tacrolimus in LDLT recipients [8,9]. We have also demonstrated that the *CYP3A5*1* allele in the native intestine as well as the graft liver is associated with the reduced concentration/dose (C/D) ratio of tacrolimus in LDLT recipients [10,11].

Population pharmacokinetic analysis with the nonlinear mixed-effects modeling (NONMEM) program has been widely used to identify the covariates that significantly

influence the pharmacokinetics of tacrolimus in liver transplant patients [12–17]. We previously developed population pharmacokinetic models for tacrolimus with NONMEM in pediatric and adult patients receiving LDLT, and revealed that the clearance of tacrolimus increased with time after surgery [18,19]. In our recent study, the intestinal expression level of MDR1 mRNA was shown to have a significant effect on the initial value of oral clearance (CL/F) of tacrolimus in pediatric LDLT recipients [20]. Furthermore, the recovery of CL/F with time was demonstrated to be twice higher in patients receiving a *CYP3A5*1*-carrying graft liver (CYP3A5 expressors) than in patients with the hepatic *CYP3A5*3/*3* genotype (CYP3A5 nonexpressors) [20]. The graft size in adult LDLT recipients is inevitably smaller than the ideal liver size for the recipient's metabolic demands, whereas the graft liver in most pediatric LDLT recipients is large enough [21,22]. A small-for-size graft, in which the functional liver mass is reduced and necessary for liver regeneration, is considered as an important factor affecting the disposition of drugs including tacrolimus in adult liver transplant patients [17,23,24]. Therefore, it is likely that the major organ(s) and molecule(s) responsible for the pharmacokinetic variability of tacrolimus differ between pediatric and adult LDLT recipients, owing to the difference in size of the grafted liver.

Renal dysfunction is a frequent complication in transplant patients receiving the calcineurin inhibitors tacrolimus and cyclosporine [25]. Although there are clinical data suggesting that renal P-glycoprotein is a risk factor for nephrotoxicity of calcineurin inhibitors, conflicting results have been reported with regard to a causal relationship between the *MDR1* G2677T/A and C3435T genetic polymorphisms and nephrotoxicity [26,27]. In contrast, CYP3A5 is also expressed in the kidney, and the formation of cyclosporine and tacrolimus metabolites by renal CYP3A5 *in vitro* has been demonstrated [28,29]. Recently, decreased expression of renal CYP3A5 was reported in patients with calcineurin inhibitor-related nephrotoxicity [30]. Therefore, it can be hypothesized that CYP3A5 in the kidney has an influence on the development of nephrotoxicity induced by calcineurin inhibitors in transplant patients, probably by reducing drug accumulation within renal cells.

In this study, the impact of hepatic or intestinal *MDR1*, *CYP3A4*, and *CYP3A5* genes on the CL/F of tacrolimus in *de novo* adult LDLT recipients was examined by using a population pharmacokinetic approach. Furthermore, the development of renal dysfunction within 1 year after transplantation was analyzed in relation to the donor's and recipient's *CYP3A5* genotypes.

Methods

Patients and ethics

A total of 60 *de novo* Japanese adult liver transplant patients receiving tacrolimus were enrolled in this study. All patients underwent LDLT between May 2005 and March 2006 at the Department of Surgery, Kyoto University Hospital, Kyoto, Japan. Patients were eligible for the study if pharmacogenomic data for both donors and recipients were available. Patients treated with the concomitant use of potent inducers or inhibitors of CYP3A and P-glycoprotein were excluded, but patients receiving intravenous high-dose corticosteroids for the treatment of a subclinical rejection episode were not excluded. In addition, the use of low-dose fluconazole for prophylaxis of fungal infections was allowed. This study was conducted in accordance with the Declaration of Helsinki and its amendments, and the protocol was approved by the Ethics Committee of Kyoto University Graduate School and Faculty of Medicine. Written informed consent was obtained from each patient.

Immunosuppressive therapy

After liver transplantation, we started tacrolimus-based immunosuppressive therapy combined with corticosteroids. Tacrolimus (Prograf, Astellas Pharma Inc., Tokyo, Japan) was orally administered at 0.05 mg/kg/day twice daily (at 09 : 00 and 21 : 00 h). The dosage was adjusted to achieve the target trough level, which was set at between 10 and 15 ng/ml during the first 2 weeks, at approximately 10 ng/ml thereafter, and at between 5 and 10 ng/ml starting in the second month. Methylprednisolone (10 mg/kg) was intravenously administered at the time of graft reperfusion, and then the dosage was gradually reduced, and the patients were switched to oral prednisolone 1 week after surgery. The dosage was gradually tapered off and discontinued between 3 and 6 months after the transplant if clinically possible.

Tacrolimus assay

Blood samples for the routine TDM of tacrolimus trough levels were collected into ethylenediaminetetra-acetic acid-containing tubes before the morning dose (at 08 : 00 h) starting on postoperative day 2. The concentration of tacrolimus in whole blood was determined by a microparticle enzyme immunoassay method using an IMx analyzer (Abbott Japan, Tokyo, Japan) on the day of blood collection [31]. Clinical laboratory test markers were simultaneously measured in the morning during hospitalization.

Pharmacogenomic analysis

Tissue samples (approximately 1 mm^3) of the upper jejunum and liver were obtained from part of the Roux-en-Y limb for biliary reconstruction and the biopsy specimens for histopathological examination of the graft liver at surgery, respectively.

For the *MDR1* polymorphisms, we previously clarified that the G2677T/A and C3435T polymorphisms did not influence the mRNA expression level in enterocytes or

the C/D ratio of tacrolimus in LDLT recipients [32]. Regarding the *CYP3A4* mutant allele, the *CYP3A4*1B* allele is very rare in Asians and seems not to be responsible for the variability in the disposition of cyclosporine [33]. In contrast, the *CYP3A5*3* allele resulting in a functional CYP3A5 deficiency was reported as the major mutant allele in the Japanese population [34,35]. Therefore, in this study we genotyped the *CYP3A5*3* polymorphism as described previously [11]. Briefly, genomic DNA was extracted from a homogenate of biopsy specimens of the graft liver and the intestinal mucosa or peripheral blood of recipients with MagNA Pure LC DNA Isolation kit I (Roche, Mannheim, Germany). The *CYP3A5*3* polymorphism was determined by the polymerase chain reaction (PCR)-restriction fragment length polymorphism method.

Total RNA was extracted from the homogenate from the graft liver and the intestinal mucosa with MagNA Pure LC RNA Isolation kit II (Roche) and reversed transcribed as described earlier [9]. Subsequently, the expression of MDR1, CYP3A4, and CYP3A5 mRNAs was quantified by real-time PCR using an ABI Prism 7700 Sequence Detector (Applied Biosystems, Foster, California, USA) according to a procedure described previously [10].

Population pharmacokinetic analysis

A total of 1827 blood samples collected within the first 50 days after LDLT were used for the population pharmacokinetic analysis of tacrolimus with the program NONMEM (double precision NONMEM version V level 2.1, PREDPP version III level 1.1, and NMTRAN version II level 2.1) using the first-order conditional estimation method [36]. As blood samples were collected predose in this study, the pharmacokinetics of tacrolimus after oral administration was described by a 1-compartment model with first-order elimination, and the basic pharmacokinetic parameters estimated were CL/F (l/h) and apparent volume of distribution (V/F, l). For the random error model, the interindividual variability of pharmacokinetic parameters and the residual variability between the observed and predicted concentrations were best described with an exponential error model and an additive error model, respectively.

In the model development process, a forward inclusion and backward elimination approach was used to build a regression model for CL/F. Owing to a lack of information on the distribution phase during the trough level monitoring, we did not perform a covariate analysis for the V/F of tacrolimus (V/F = θ_2). The effect of a covariate was assessed with a χ^2 test of the difference in the objective function values (OFV) calculated by NONMEM between the models with and without a covariate. If a difference in the OFV between two models [−2 log likelihood difference (−2 LLD)] was more than 3.84 ($P < 0.05$) with 1 degree of freedom on the inclusion of each covariate, the covariate was considered statistically significant.

Previously, tacrolimus clearance was shown to increase with time after liver transplantation and reach a steady state within the first month [15,20]. According to this observation, we first examined the relationship of CL/F with time after surgery by using the following cutoff model:

$$CL/F = \theta_1 + \theta_3 \times XPOD$$

if POD < CP, XPOD = POD; otherwise, XPOD = CP where θ_1 and θ_3 are the initial value of CL/F immediately after LDLT and the increase in CL/F per day, respectively; POD is postoperative days and XPOD is an arbitrary value of POD; and CP is the cutoff point for POD.

The influence of patient characteristics including demographics and clinical laboratory data on CL/F in the derived time-dependent clearance model was next examined using an exponential function, with the effect of each covariate normalized by the respective median value. At each step in the selection process, the factor showing the largest −2 LLD among significant covariates was incorporated into the cutoff model. Then, all factors that were found to be significant were reassessed, and the factor that showed the largest −2 LLD was included in the intermediate model. This step was repeated until the greatest −2 LLD was below 3.84 to obtain the full model. Throughout the covariate analysis, the precision of the parameter estimate [95% confidence interval (CI)] and the reduction in interindividual and residual variability as well as scatter plots of observed versus model-predicted concentrations were used as another indicator of the goodness-of-fit in each model. Upon the independent deletion of each covariate, a −2 LLD between the full and reduced models of more than 7.88 ($P < 0.005$) was required to retain a covariate in the final population model (model 1).

Finally, we investigated all possible relationships of CL/F in model 1 with hepatic or intestinal MDR1 and CYP3A4 mRNAs and the *CYP3A5*1* allele, by using both multiplicative and additive models. Quantitative covariates of MDR1 and CYP3A4 mRNAs were transformed into dichotomous variables (high or low) according to the median value. As the *CYP3A5* genotype can be a relevant predictor for CYP3A5 expression, the impact of the *CYP3A5*1* allele on CL/F was examined as a binary variable [expressors (**1/*1* and **1/*3*) or nonexpressors (**3/*3*)] for the CYP3A5 enzyme. In this analysis, we estimated the fractional increase in CL/F associated with high mRNA levels of MDR1 and CYP3A4 or the functional expression of CYP3A5. The statistical significance of pharmacogenomic data as a covariate for CL/F

was tested according to the approach described above to develop the final population model (model 2).

Analysis of renal dysfunction in relation to the *CYP3A5* genotype

Tacrolimus-related nephrotoxicity was defined as an initial increase in the serum creatinine (SCR) level greater than 0.5 mg/dl above the pretransplant baseline. To avoid the potential influence of preoperative renal dysfunction on the incidence of adverse events, we excluded three patients who had renal dialysis ($n = 1$) and were diagnosed with renal impairment ($n = 2$) before LDLT. A 1-year follow-up after the transplant was performed to investigate the possible association between renal dysfunction and the *CYP3A5*1* status of donors as well as recipients. The medical records of each patient were reviewed for abstraction of SCR values, which had been reported on the day of regular hospital visits (3, 6, 9, and 12 months after transplantation) for outpatients, as well as throughout the hospitalization for inpatients. Data available near the intended time points were used to calculate the average values for dose requirements and trough blood concentrations of tacrolimus.

Statistical analysis

The statistical significance of differences in parametric and nonparametric values between two groups was analyzed with the unpaired *t*-test and the Mann–Whitney *U*-test, respectively. Hardy–Weinberg equilibrium for genotype frequency was examined by the χ^2 test. The proportion of patients with renal dysfunction was determined with the Kaplan–Meier method, and the log-rank test was used to examine the significance of differences between two curves. *P* value of less than 0.05 was considered statistically significant.

Results

Patients and pharmacogenomic data

The demographics and clinical laboratory data for the study population are shown in Table 1. The most common primary disease leading to LDLT was cirrhosis (56/60, 93.3%). The median value of the graft-to-recipient weight ratio (GRWR) was significantly lower than in our earlier study of 130 pediatric LDLT recipients [20] (1.1 vs. 2.6%, $P < 0.05$, Mann–Whitney *U*-test). Although most of the blood tacrolimus concentrations were maintained within the therapeutic window (5–15 ng/ml), the trough levels were variable at around the target range, especially during the first week after transplantation (Fig. 1).

The pharmacogenomic data for this study population are summarized in Table 2. The expression profiles of MDR1 and CYP3A4 mRNAs in the native intestine as well as the graft liver were generally comparable with those reported previously for pediatric cases of LDLT [20]. The CYP3A5 mRNA content was significantly correlated with the *CYP3A5* genotype in both tissues ($P < 0.05$). The median mRNA level of CYP3A5 in the native intestine was similar to that in pediatric LDLT recipients [20] (0.24 vs. 0.11 amol/μg total RNA, respectively). The median

Table 1 Characteristics of the study population ($n=60$)

Demographics	
Sex (male/female)	29/31
Age (year)	55 (29–70)
Body weight (kg)	57 (41–85)
Graft weight (g)	695 (425–935)
Graft-to-recipient weight ratio (%)	1.1 (0.7–2.1)
Primary disease	
Cirrhosis	56
Hepatitis C virus infection	24
Hepatitis B virus infection	19
Primary biliary cirrhosis	6
Alcoholic cirrhosis	3
Unknown cirrhosis	4
Others	4
Donor (male/female)	32/28
Donor age (year)	47 (21–66)
Clinical laboratory data[a]	
Hematocrit (%) (33.7–49.8)	28.0 (19.8–45.9)
Total protein (g/dl) (6.3–8.1)	6.6 (4.6–8.5)
Serum albumin (g/dl) (3.9–5.1)	3.1 (2.2–4.4)
Total bilirubin (mg/dl) (0.3–1.3)	2.9 (0.4–38.1)
AST (IU/l) (13–33)	51 (23–173)
ALT (IU/l) (8–42)	29 (7–129)
γ-Glutamyl transpeptidase (IU/l) (9–54)	36 (11–873)
Serum creatinine (mg/dl) (0.6–1.1)	0.8 (0.3–1.9)
Blood urea nitrogen (mg/dl) (8–22)	16 (4–82)
Pharmacokinetic data of tacrolimus[b]	
Number of samples	1827
Number of samples per patient	30 (13–49)
Dose (mg/day)	3.0 (0.2–16.0)
Trough concentration (ng/ml)	8.6 (1.6–26.9)

Data are expressed as a number or median (range).
ALT, alanine aminotransferase; AST, aspartate aminotransferase; LDLT, living-donor liver transplantation.
[a]Range in parentheses indicates reference data at Kyoto University Hospital, Kyoto, Japan, for normal adult men.
[b]Dose and trough concentration are based on all data from the first 50 days after LDLT.

Fig. 1

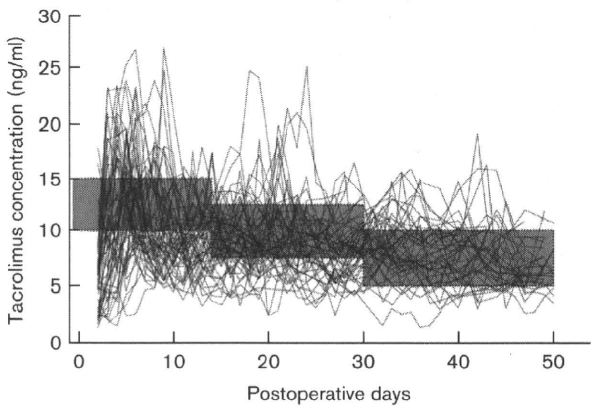

Tacrolimus trough concentrations in whole blood vs. postoperative days for all recipients ($n=60$). Data from the same patient are connected with a line. The closed area shows the target range in each postoperative period (10–15 ng/ml during the first 2 weeks, approximately 10 ng/ml thereafter, and 5–10 ng/ml starting in the second month).

Table 2 Pharmacogenomic data for the study population ($n=60$)

	Recipient	Donor
	Native intestine	Graft liver
Expression level		
MDR1 mRNA (amol/μg total RNA)	0.15 (0.01–1.1)	0.81 (0.40–2.9)
CYP3A4 mRNA (amol/μg total RNA)	3.5 (0.001–16)	50 (11–130)
CYP3A5 mRNA (amol/μg total RNA)	0.24 (0.001–2.5)	1.6 (0.26–23)
**1/*1* and **1/*3* (amol/μg total RNA)	0.73[a] (0.001–2.5)	8.4[a] (3.9–23)
**3/*3* (amol/μg total RNA)	0.16 (0.001–1.5)	1.1 (0.26–6.4)
Genotype frequency[b]		
*CYP3A5*1/*1*	3 (5.0%)	1 (1.7%)
*CYP3A5*1/*3*	17 (28.3%)	23 (38.3%)
*CYP3A5*3/*3*	40 (66.7%)	36 (60.0%)

Data are expressed as the median (range) for expression level and as the number of patients (percent) for genotype frequency.
[a]$P<0.05$, significant difference in the distribution from the *CYP3A5*3/*3* group (Mann–Whitney *U*-test).
[b]Genotype frequency was not significantly different from that predicted by Hardy–Weinberg equilibrium ($P>0.05$ for recipient and donor, χ^2 test).

(range) expression level of CYP3A5 mRNA in the graft liver was 1.6 (0.26–23) amol/μg total RNA, which was also comparable with that in pediatric LDLT recipients [20] [1.0 (0.10–10) amol/μg total RNA]. The genotype frequencies of the *CYP3A5*3* polymorphism for both donors and recipients were in Hardy–Weinberg equilibrium, and well consistent with the earlier report for pediatric cases of LDLT [20].

Development of a time-dependent clearance model for tacrolimus

The OFV of the basic model without any covariate was 7200.22. Initially, we tested allometric scaling of CL/F and V/F in the basic model by using body weight. The inclusion of body weight, however, did not significantly decrease the OFV. In addition, neither age nor sex showed any correlation with the individual Bayesian estimates for CL/F and V/F, which were obtained using the post-hoc option of NONMEM. Therefore, the basic model was used for the subsequent analysis.

In the plot of weighted residuals against postoperative days, the basic model systematically underestimated blood tacrolimus concentrations for the first few weeks after transplantation. To describe the postoperative recovery of CL/F after LDLT, the factor of postoperative days was adopted as a covariate for the cutoff model. We examined three different cutoff points for postoperative days (7, 14, and 21) and confirmed that the best fit was obtained using 14 (OFV = 6079.49). Accordingly, a time-dependent clearance model for tacrolimus was developed, where CL/F increased linearly after LDLT but did not change with time after postoperative day 14.

Influence of patient characteristics on tacrolimus CL/F

We investigated the potential influence of the graft liver (GRWR) and clinical laboratory data on CL/F in the derived cutoff model. In the first selection step, GRWR did not significantly reduce the OFV (−2 LLD = 1.00), whereas the effect of SCR showed the largest improvement of fit (−2 LLD = 57.61) and was incorporated into the cutoff model. The effects of total bilirubin (TBIL) and serum albumin (ALB) were included in the intermediate model in the second and third selection steps, respectively. In the fourth selection step, a significant improvement of fit was no longer observed to obtain the full model. No covariate was excluded by backward elimination to derive the following final population model for CL/F (model 1):

$$\mathrm{CL/F} = (0.340 + 0.964 \times \mathrm{XPOD}) \times \mathrm{EXP}(-0.423 \times \mathrm{SCR}/0.8) \times \mathrm{EXP}(-0.0399 \times \mathrm{TBIL}/2.9) \times \mathrm{EXP}(0.476 \times \mathrm{ALB}/3.1)$$

(if POD < 14, then XPOD = POD; otherwise, XPOD = 14).

Influence of pharmacogenomic data on tacrolimus CL/F

We examined the contribution of pharmacogenomic data on CL/F in model 1, using the mRNA levels of MDR1 and CYP3A4 as well as the *CYP3A5*1* genotype. As shown in Table 3, the OFV was markedly decreased by more than 10 U from model 1 in the first selection step, when including the effects of the intestinal *CYP3A5*1* allele with multiplicative and additive models (−2 LLD = 10.39 and 10.84, respectively), as well as the effect of the intestinal CYP3A4 mRNA by an additive function (−2 LLD = 10.98). We selected the multiplicative model for the intestinal *CYP3A5*1* allele, which had the smallest interindividual variability of CL/F ($\omega_{CL/F} = 47.2\%$). In the second selection step, the influence of the mRNA levels of MDR1 and CYP3A4 in the native intestine improved likewise the fit of the intermediate model (−2 LLD = 9.50 and 9.74, respectively). We chose the effect of the intestinal MDR1 mRNA, showing the smaller interindividual variability of CL/F compared with that of CYP3A4 ($\omega_{CL/F} = 46.2$ vs. 48.1%, respectively). In the third selection step, the effect of the hepatic *CYP3A5*1* allele was found to be significant (−2 LLD = 5.56). This covariate, however, was excluded by backward elimination and the final population model (model 2, Table 4) was developed. Although the residual variability and the interindividual variability of V/F did not decrease in model 2 compared with model 1, the interindividual variability of CL/F could be lowered to 46.2% in model 2 from 51.8% in model 1 (Table 4). Although the scatter plot of population prediction with model 2 vs. observed concentration showed a marked deviation (Fig. 2a), the Bayesian method using individual blood concentration data provided more accurate and less biased predictions of blood tacrolimus concentrations (Fig. 2b).

Figure 3 shows that the population mean predictions of CL/F based on the final model 2 in a typical patient having the median values of SCR, TBIL, and ALB. The increase in CL/F with postoperative days was 1.47 times higher (95% CI, 1.17–1.77 times, $P < 0.005$) in patients

Table 3 Summary of model building process for tacrolimus CL/F using pharmacogenomic data

Models[a]	Covariates[b]	−2 LLD[c] First selection	−2 LLD[c] Second selection	−2 LLD[c] Third selection
Multiplicative model $CL/F=(\theta_1+\theta_3\times XPOD)\times EXP(-\theta_4\times SCR/0.8)\times EXP(-\theta_5\times TBIL/2.9)\times EXP(\theta_6\times ALB/3.1)\times\theta_7^{FLAG}$	Donor/graft liver			
	MDR1 mRNA	0.15 (51.7%)		
	CYP3A4 mRNA	0.58 (51.5%)		
	*CYP3A5*1* allele	4.84 (49.6%)[d]	4.17 (45.5%)[d]	5.56 (46.0%)*
	Recipient/native intestine			
	MDR1 mRNA	2.11 (50.9%)		
	CYP3A4 mRNA	0.46 (51.6%)		
	*CYP3A5*1* allele	10.39 (47.2%)[d,e]		
Additive model $CL/F=(\theta_1+\theta_3\times XPOD)\times EXP(-\theta_4\times SCR/0.8)\times EXP(-\theta_5\times TBIL/2.9)\times EXP(\theta_6\times ALB/3.1)+\theta_7\times FLAG$	Donor/graft liver			
	MDR1 mRNA	1.43 (51.8%)		
	CYP3A4 mRNA	0.19 (51.7%)		
	*CYP3A5*1* allele	0.01 (51.8%)		
	Recipient/native intestine			
	MDR1 mRNA	8.00 (51.1%)[d]	9.50 (46.2%)[d,e]	
	CYP3A4 mRNA	10.98 (52.2%)[d]	9.74 (48.1%)[d]	3.08 (46.5%)
	*CYP3A5*1* allele	10.84 (49.2%)[d]		

ALB, serum albumin; FLAG, indicator variable having 0 or 1; −2 LLD, −2 log likelihood difference [a reduction of the objective function value (OFV)]; POD, postoperative days; SCR, serum creatinine; TBIL, total bilirubin; XPOD, an arbitrary value of POD.
[a]Model 1 [$CL/F=(\theta_1+\theta_3\times XPOD)\times EXP(-\theta_4\times SCR/0.8)\times EXP(-\theta_5\times TBIL/2.9)\times EXP(\theta_6\times ALB/3.1)$ (if POD <14, XPOD=POD; otherwise, XPOD=14); $V/F=\theta_2$; OFV=5954.27] was used as a basic model to develop a refined population model including pharmacogenomic covariates (model 2).
[b]A high expressor of MDR1 and CYP3A4 was identified by an mRNA level greater than the respective median value (shown in Table 2). If the donor or recipient was a high expressor of MDR1 or CYP3A4 mRNA, FLAG=1; otherwise, FLAG=0. If the donor or recipient carried the *CYP3A5*1* allele, FLAG=1; otherwise, FLAG=0.
[c]Interindividual variability of CL/F is presented in parentheses beside the value of −2 LLD.
[d]$P<0.05$, significant difference in the goodness-of-fit between models with and without a covariate.
[e]The covariate showing the smallest interindividual variability of CL/F among significant covariates that yielded a close −2 LLD was incorporated into the intermediate model.

Table 4 Final population pharmacokinetic estimates for tacrolimus in adult LDLT patients

Parameters	Model 1[a]	Model 2[b]
Fixed effects		
θ_1 (l/h)	0.340 (0.0928–0.587)	–
θ_2 (l)	644 (531–757)	631 (514–748)
θ_3 (l/h/day)	0.964 (0.612–1.32)	0.784 (0.464–1.10)
θ_4	0.423 (0.257–0.599)	0.443 (0.269–0.617)
θ_5	0.0399 (0.0243–0.0555)	0.0425 (0.0272–0.0578)
θ_6	0.476 (0.196–0.756)	0.529 (0.229–0.829)
θ_7	–	1.47 (1.17–1.77)
θ_8 (l/h)	–	1.06 (0.160–1.96)
Random effects		
$\omega_{CL/F}$ (%)	51.8 (39.3–61.7)	46.2 (35.8–54.6)
$\omega_{V/F}$ (%)	66.5 (53.7–77.2)	68.0 (54.3–79.4)
σ (ng/ml)	2.73 (2.53–2.92)	2.73 (2.52–2.92)

Data are expressed as the mean value (95% CI).
[a]Model 1 was described with the following equations: $CL/F=(\theta_1+\theta_3\times XPOD)\times EXP(-\theta_4\times SCR/0.8)\times EXP(-\theta_5\times TBIL/2.9)\times EXP(\theta_6\times ALB/3.1)$ (if POD <14, then XPOD=POD; otherwise, XPOD=14) and $V/F=\theta_2$.
[b]Model 2 was described with the following equations: $CL/F=\theta_8\times MDR1+\theta_3\times XPOD\times EXP(-\theta_4\times SCR/0.8)\times EXP(-\theta_5\times TBIL/2.9)\times EXP(\theta_6\times ALB/3.1)\times\theta_7^{CYP3A5}$ (if POD <14, then XPOD=POD; otherwise, XPOD=14; if the recipient was a *CYP3A5*1* allele carrier, then CYP3A5=1; otherwise, 0; if the intestinal MDR1 mRNA level >0.15 amol/μg total RNA, then MDR1=1; otherwise, 0) and $V/F=\theta_2$.

Fig. 2

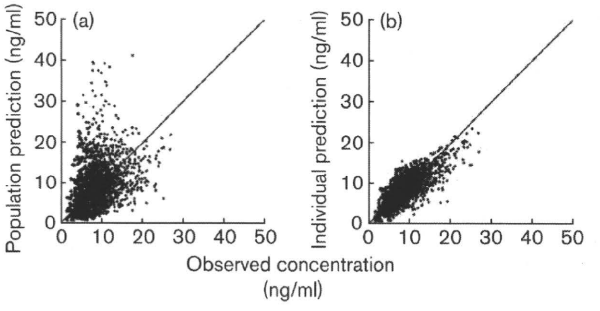

Scatter plots of observed tacrolimus concentrations vs. population predictions (a) and individual predictions by the Bayesian method with the final model 2 (b). The solid line shows the line of identity.

carrying the intestinal *CYP3A5*1* allele than in patients with the *CYP3A5*3/*3* genotype in enterocytes (Fig. 3 and Table 4). Furthermore, the higher expression of intestinal MDR1 mRNA (>0.15 amol/μg total RNA) resulted in the augmentation of CL/F by 1.06 l/h (95% CI, 0.160–1.96 l/h, $P<0.005$) (Fig. 3 and Table 4).

The longitudinal influence of the enterocyte *CYP3A5*1* allele on CL/F was examined by dividing the immediate postoperative period into seven different weeks. The individual CL/F estimates on the last day in each week were obtained with the Bayesian method by using blood concentration data available during the respective week and the final model 2. The significant influence of the intestinal *CYP3A5*3* polymorphism on the individual CL/F estimates was confirmed until postoperative day 28, but thereafter the distribution of the individual CL/F

Fig. 3

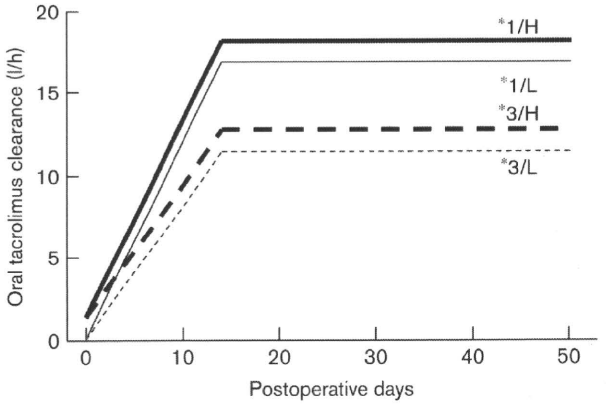

Time-dependent changes in population mean estimates of oral tacrolimus clearance obtained with the final model 2 during the first 50 postoperative days. The bold and thin solid lines represent the tacrolimus CL/F in a typical patient (serum creatinine, 0.8 mg/dl; total bilirubin, 2.9 mg/dl; serum albumin, 3.1 mg/dl) carrying the intestinal *CYP3A5*1* allele with high (*1/H) and low (*1/L) intestinal MDR1 mRNA levels, respectively. The bold and thin dotted lines indicate the tacrolimus CL/F in a typical patient having the intestinal *CYP3A5*3/*3* genotype with high (*3/H) and low (*3/L) intestinal MDR1 mRNA levels, respectively.

Fig. 4

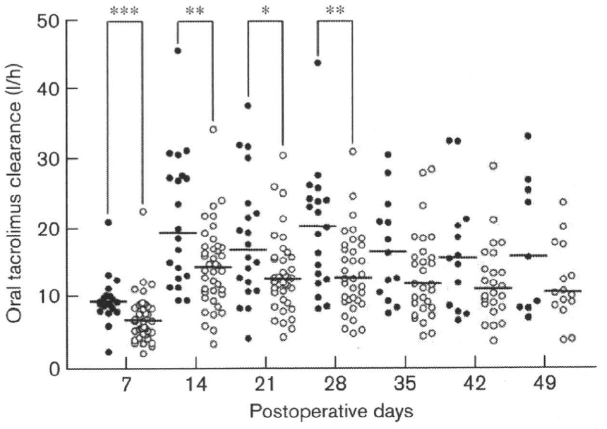

The influence of intestinal *CYP3A5*1* genotype on the individual Bayesian estimates of oral tacrolimus clearance throughout the first seven weeks after LDLT. The closed and open circles represent the data from patients carrying the *CYP3A5*1* allele (CYP3A5 expressors) and patients with the *CYP3A5*3/*3* genotype (CYP3A5 nonexpressors) in the native intestine, respectively. Each bar indicates the median value. $*P<0.05$, $**P<0.01$, $***P<0.001$, significant difference between two groups (Mann–Whitney *U*-test). LDLT, living-donor liver transplantation.

estimates was not significantly different between patients with and without the intestinal *CYP3A5*1* allele (Fig. 4).

Tacrolimus exposure and nephrotoxicity according to the *CYP3A5* genotype

Table 5 shows the daily dose and exposure parameters of tacrolimus over a 1-year period after LDLT. Trough blood concentration (C_0) throughout the follow-up period did not differ between expressors (**1/*1* and **1/*3*) and nonexpressors (**3/*3*) of CYP3A5 in donors as well as recipients. On day 7, bodyweight-normalized dose and C/D ratio were significantly affected by the *CYP3A5*1* allele in both donors and recipients, whereas the *CYP3A5*1* allele in recipients alone significantly influenced these two parameters on day 14. After the first month, the *CYP3A5*1* allele in donors but not in recipients had a significant effect on tacrolimus dose and C/D ratio. These results were not altered when three patients with preoperative renal dysfunction were excluded from analysis.

The cumulative incidence of renal dysfunction within 1 year after transplantation was not affected by the *CYP3A5*1* allele in donors [**1/*1* and **1/*3* vs. **3/*3*: 8/23 (35%) vs. 13/34 (38%), $P = 0.81$] (Fig. 5a). In contrast, the *CYP3A5*3/*3* genotype in recipients was significantly associated with the increased incidence of tacrolimus-related nephrotoxicity [**1/*1* and **1/*3* vs. **3/*3*: 3/18 (17%) vs. 18/39 (46%), $P < 0.05$; hazard ratio (95% CI), 3.16 (1.01–6.16)] (Fig. 5b).

Discussion

Population pharmacokinetic and pharmacogenomic analysis with the NONMEM program has advantages in identifying statistically significant covariates among various factors as well as in determining the impact of genomic variation on the clinical pharmacokinetics of drugs [20,37–40]. Figure 1 shows that the difficulty in maintaining the blood tacrolimus concentrations within the target range despite the daily adjustment of oral dosage based on TDM, especially in the first week after LDLT. Therefore, we attempted to establish a more accurate population pharmacokinetic model for tacrolimus by using pharmacogenomic information and clinical data obtained during the initial posttransplant period. In this study, we have first clarified that the *CYP3A5*1* allele as well as the MDR1 mRNA level in enterocytes is an important determinant for the CL/F of tacrolimus in adult recipients early after LDLT.

In a time-dependent clearance model for tacrolimus, the time needed for CL/F to reach a steady state was estimated as 14 days. In pediatric LDLT recipients, the recovery of CL/F was calculated to take 21 days [20]. These results suggest that the tacrolimus dose in pediatric patients should be increased gradually for the first 3 weeks after LDLT, whereas adult patients would require dose escalation for the initial 2 weeks. In the covariate analysis, CL/F was found to be related to SCR, TBIL, and ALB. These factors have been demonstrated as significant covariates for tacrolimus clearance in other

Table 5 Tacrolimus dose and exposure parameters over time in adult LDLT patients according to donor's and recipient's *CYP3A5* genotypes

	Donor		Recipient	
Time posttransplantation	**3/*3* ($n=36$)	**1/*1* and **1/*3* ($n=24$)	**3/*3* ($n=40$)	**1/*1* and **1/*3* ($n=20$)
Day 7				
Daily dose (mg/kg)	0.037 ± 0.025	0.057 ± 0.030[a]	0.041 ± 0.030	0.054 ± 0.023[a]
C_0 (ng/ml)	10.8 ± 4.2	11.1 ± 3.8	11.1 ± 3.9	10.6 ± 4.2
C/D ratio [(ng/ml)/(mg/kg)]	454 ± 320	217 ± 118[a]	414 ± 324	256 ± 137[a]
Day 14				
Daily dose (mg/kg)	0.057 ± 0.032	0.074 ± 0.051	0.054 ± 0.034	0.083 ± 0.049[a]
C_0 (ng/ml)	9.5 ± 3.1	9.5 ± 3.5	9.7 ± 3.3	9.1 ± 3.0
C/D ratio [(ng/ml)/(mg/kg)]	228 ± 148	222 ± 188	251 ± 167	178 ± 148[a]
Month 1				
Daily dose (mg/kg)	0.051 ± 0.033	0.086 ± 0.046[a]	0.061 ± 0.042	0.082 ± 0.043
C_0 (ng/ml)	8.5 ± 2.7	8.9 ± 2.2	8.4 ± 2.4	9.1 ± 2.6
C/D ratio [(ng/ml)/(mg/kg)]	226 ± 154	159 ± 126[a]	201 ± 134	184 ± 167
Month 3				
Daily dose (mg/kg)	0.043 ± 0.024	0.061 ± 0.034[a]	0.046 ± 0.031	0.059 ± 0.024
C_0 (ng/ml)	7.7 ± 2.1	7.0 ± 2.7	7.4 ± 2.2	7.5 ± 2.7
C/D ratio [(ng/ml)/(mg/kg)]	227 ± 131	145 ± 99[a]	209 ± 122	162 ± 127
Month 6				
Daily dose (mg/kg)	0.034 ± 0.019	0.065 ± 0.038[a]	0.042 ± 0.030	0.053 ± 0.032
C_0 (ng/ml)	6.5 ± 2.0	6.4 ± 2.8	6.5 ± 2.3	6.5 ± 2.3
C/D ratio [(ng/ml)/(mg/kg)]	248 ± 132	135 ± 110[a]	216 ± 124	182 ± 157
Month 9				
Daily dose (mg/kg)	0.033 ± 0.018	0.074 ± 0.057[a]	0.045 ± 0.044	0.058 ± 0.038
C_0 (ng/ml)	5.7 ± 2.0	6.6 ± 2.3	5.9 ± 2.1	6.4 ± 2.2
C/D ratio [(ng/ml)/(mg/kg)]	216 ± 162	139 ± 116[a]	191 ± 109	178 ± 154
Month 12				
Daily dose (mg/kg)	0.031 ± 0.019	0.057 ± 0.033[a]	0.037 ± 0.026	0.049 ± 0.030
C_0 (ng/ml)	5.8 ± 1.5	6.3 ± 2.4	6.1 ± 2.0	5.8 ± 1.7
C/D ratio [(ng/ml)/(mg/kg)]	256 ± 178	157 ± 124[a]	239 ± 174	183 ± 149

Data are expressed as the mean ± SD.
C_0, trough blood concentration; C/D, dose-adjusted trough blood concentration.
[a]$P<0.05$, significant difference in the mean value from the *CYP3A5*3/*3* group (unpaired *t*-test).

Fig. 5

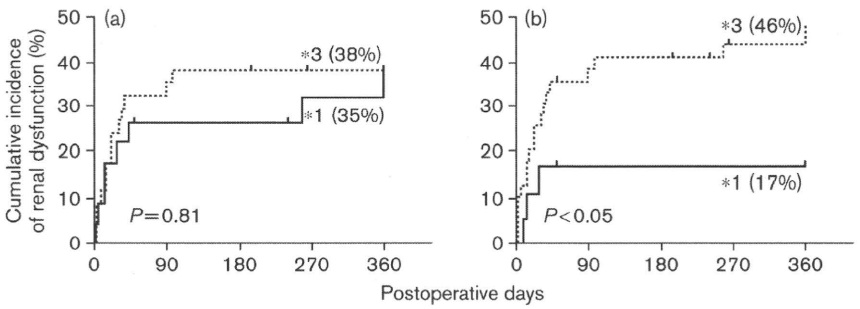

Cumulative incidence of renal dysfunction according to the *CYP3A5* genotypes of donors (a) and recipients (b). Tacrolimus-related nephrotoxicity was defined as an initial increase in the serum creatinine level greater than 0.5 mg/dl above the pretransplant baseline. The solid and dotted curves represent patients carrying the *CYP3A5*1* allele (CYP3A5 expressors, *1) and patients with the *CYP3A5*3/*3* genotype (CYP3A5 nonexpressors, *3), respectively. Small vertical tick marks indicate censored patients (end of follow-up). *P* values were determined with the Kaplan–Meier method and the log-rank test.

studies [13,15–17,19]. As tacrolimus undergoes almost no renal elimination (> 95% of dose excreted into bile) [4], indirect mechanisms may be relevant to the inverse correlation between SCR and CL/F. It was reported that tacrolimus clearance increased with time after kidney transplantation [41,42]. From this finding, one possible explanation for the association between SCR and CL/F is that renal failure may result in impaired hepatic metabolism of tacrolimus through the decrease of hepatic CYP3A activity. This mechanism may have occurred in patients who suffered from the hepatorenal syndrome. On the basis of the final model 1 (Table 4), transplant physicians can calculate the tacrolimus dose for an individual patient to achieve the target trough levels early after LDLT, taking renal as well as hepatic function into consideration on each postoperative day.

Limited information is available on the role of enterocyte CYP3A5 in the clinical pharmacokinetics of drugs. Mouly *et al.* [43] studied the pharmacokinetics of saquinavir in

healthy participants and suggested that the increase in the CL/F of saquinavir associated with the *CYP3A5*1* genotype does not reflect intestinal CYP3A5 expression but reflects the contribution of hepatic CYP3A5. Moreover, it has been revealed that patients with a liver graft carrying the *CYP3A5*1* allele had a lower C/D ratio of tacrolimus than patients with a *CYP3A5*3/*3*-carrying graft liver [10,44,45]. Recently, we have demonstrated that the recovery of tacrolimus CL/F with time after LDLT was increased in pediatric patients with a *CYP3A5*1*-carrying graft liver, but not with the *CYP3A5*1* allele in the native intestine [20]. Interestingly, in this study, adult patients carrying the *CYP3A5*1* allele in the native intestine had a 1.47 times higher (95% CI, 1.17–1.77 times) recovery of tacrolimus CL/F with time than those with the intestinal *CYP3A5*3/*3* genotype (Fig. 3 and Table 4). These findings were consistent with our previous observation that the tacrolimus C/D ratio was significantly lower in recipients with the intestinal *CYP3A5*1/*1* genotype than in patients with the *CYP3A5*3/*3* genotype in enterocytes during the first month after LDLT [11]. One possible explanation for the organ-specific effects of the *CYP3A5*1* genotype on tacrolimus CL/F in pediatric and adult LDLT recipients is the difference in functional graft size between the two populations, who had comparable levels of CYP3A5 mRNA in the native intestine as well as the graft liver at transplantation. Specifically, the native intestine, where CYP3A5 is polymorphically expressed, may more significantly contribute to the first-pass effect of tacrolimus in adult patients receiving a small-for-size graft liver than pediatric patients with an adequate-sized graft.

A significant impact of the intestinal *CYP3A5*1* allele on the individual CL/F estimates was observed during the first 4 weeks of transplant (Fig. 4), which was consistent with our previous results mentioned above [11]. After the first month, the influence of the *CYP3A5*1* genotype in enterocytes was no longer statistically significant (Fig. 4). As shown in Table 5, the intestinal *CYP3A5*1* allele was reported to significantly relate with the increased dose requirements and reduced C/D ratio of tacrolimus on postoperative days 7 and 14 in a univariate analysis, which supports a more important role for enterocyte CYP3A5 in first-pass metabolism than hepatic CYP3A5 immediately after LDLT. The individual Bayesian estimates of CL/F varied widely in patients both with and without the *CYP3A5*1* allele in enterocytes (Fig. 4). To explore the reason for the diversity observed in patients carrying the intestinal *CYP3A5*1* allele (CYP3A5 expressors), we compared the individual CL/F estimates with the mRNA levels of CYP3A5 in the native intestine. No significant correlation, however, was found between them (data not shown). Taking these findings into consideration, the intestinal *CYP3A5*3* polymorphism may be an important determinant for the variability of tacrolimus CL/F in adult LDLT recipients during the first month, although the enterocyte CYP3A5 mRNA level would not predict the interindividual difference in tacrolimus CL/F. Notably, the hepatic but not intestinal *CYP3A5*1* allele significantly influenced tacrolimus dose and C/D ratio throughout the 1-year posttransplant period after the first month (Table 5), suggesting that the major organ influencing tacrolimus disposition changes from the native intestine in the early phase to the graft liver in the stable phase, with the recovery of metabolic function in the liver. From these findings, the impact of enterocyte CYP3A5 on tacrolimus CL/F may be particular to adult LDLT recipients early after surgery, whereas a significant effect of hepatic CYP3A5 on tacrolimus disposition could be a general feature of stable liver transplant patients.

The higher level of MDR1 mRNA in the native intestine led to the significant increase in CL/F (Fig. 3 and Table 4), which was consistent with our previous finding that the initial CL/F was 1.80-fold higher in pediatric LDLT recipients with a high MDR1 mRNA level than those with a low MDR1 mRNA level in enterocytes [20]. These results support the important role of enterocyte P-glycoprotein in the first-pass effect of tacrolimus during the immediate posttransplant period in both pediatric and adult patients receiving LDLT. Taking the intestinal *CYP3A5*1* genotype and MDR1 mRNA level into account, the interindividual variability of CL/F was reduced to 46.2% in the final model 2 from 51.8% in model 1 (Table 4). Consequently, these genotype/phenotype characteristics of adult LDLT recipients could account for approximately 6% of the variation in tacrolimus CL/F. The interindividual and residual variability unexplained in model 2 is still large (Table 4), and may have partly resulted from the concomitant use of inhibitors or inducers of CYP3A and P-glycoprotein such as azole antifungal agents and corticosteroids. A low-dose oral fluconazole (100 mg/day) was used for the prophylaxis of fungal infections in this study. As fluconazole is a less potent inhibitor of CYP3A4 [46], drug–drug interaction between tacrolimus and fluconazole seems not to be responsible for the marked variability in CL/F. The study population included patients receiving intravenous high-dose corticosteroids for the treatment of an acute rejection episode. Corticosteroids have been known to increase tacrolimus clearance, probably by induction of CYP3A4 [4]. Therefore, corticosteroid dose may have contributed to the interindividual variation in the CL/F of tacrolimus.

We previously showed that blood tacrolimus concentrations could be predicted with the Bayesian method 2 weeks after LDLT, when liver function has become stable [47]. Furthermore, our recent study in pediatric LDLT recipients demonstrated that Bayesian forecasting

with the population pharmacokinetic model including genotype/phenotype information provided accurate and less biased predictions of blood tacrolimus concentrations during the first week after surgery [20]. Although the variability of CL/F associated with the intestinal *CYP3A5* genotype and MDR1 mRNA level was relatively small (about 6%), the Bayesian predictions were generally well consistent with the observed concentrations of tacrolimus (Fig. 2b). On the basis of these findings, Bayesian approach-guided dosing with the final model 2 might assist in modifying the maintenance dose of tacrolimus within the early phase as well as the stable phase of transplant. For the care of adult LDLT recipients with the *CYP3A5*1* allele and high MDR1 mRNA levels in enterocytes, a higher dose of tacrolimus should be considered during hospitalization to maintain similar trough concentrations to those in patients with the intestinal *CYP3A5*3/*3* genotype and low MDR1 mRNA levels, owing to the marked difference in tacrolimus CL/F (Fig. 3). Further prospective analysis should be performed to clarify the clinical relevance of a genome-based population pharmacokinetic model for tacrolimus to the reduction of the variability in drug exposure after LDLT.

Interestingly, the cumulative incidence of renal dysfunction over the first year after transplantation was significantly related to the recipient's but not donor's *CYP3A5*1* genotype, whereas similar tacrolimus exposure (C_0) was achieved in expressors and nonexpressors of CYP3A5 (Fig. 5 and Table 5). This result may indicate that CYP3A5 in the kidney plays a protective role in the development of renal dysfunction, probably by reducing exposure of renal cells to tacrolimus. Recently, Kuypers *et al.* [48] suggested that the *CYP3A4*1/CYP3A5*1* and *CYP3A4*1B/CYP3A5*1* genotypes in recipients are associated with the more frequent development of biopsy-proven tacrolimus-related nephrotoxicity within 5 years after kidney transplantation, possibly as a result of higher concentrations of toxic metabolites. They, however, did not examine the potential association with the genotypes in donor kidney. Therefore, we could not clarify the reasons for the discrepancy with the present results. On the basis of our findings, in adult LDLT recipients with the *CYP3A5*3/*3* genotype, the setting of lower target tacrolimus concentrations could lead to less frequent nephrotoxicity, without compromising immunosuppression by introducing or increasing doses of other immunosuppressive drugs such as mycophenolate mofetil. Further studies are needed to investigate renal tissue concentrations as well as nephrotoxicity profiles of tacrolimus and its metabolites such as 13-*O*-desmethyltacrolimus.

In conclusion, we have statistically demonstrated that the MDR1 mRNA level and the *CYP3A5*3* polymorphism in the native intestine contribute to the interindividual difference in the CL/F of tacrolimus in adult patients early after LDLT. In contrast, in the stable phase after transplantation, it is likely that the major organ and molecule that have a significant influence on the tacrolimus CL/F would be changed to hepatic CYP3A5 from intestinal MDR1/CYP3A5. Furthermore, the *CYP3A5*3/*3* genotype in adult LDLT recipients may predispose them to the nephrotoxicity associated with tacrolimus. Understanding these pharmacogenomic properties of tacrolimus will help to establish a more accurate and safe dosage regimen in *de novo* patients receiving LDLT.

Acknowledgements

This study was supported in part by the 21st Century COE Program 'Knowledge Information Infrastructure for Genome Science', by a Grant-in-Aid from the Japan Health Sciences Foundation 'Research on Health Sciences Focusing on Drug Innovation', by a Grant-in-Aid for Scientific Research from the Ministry of Education, Culture, Sports, Science, and Technology of Japan, by a Grant-in-Aid from the Uehara Memorial Foundation, and by a Grant-in-Aid from the Japan Research Foundation for Clinical Pharmacology. K.H. is supported as a Research Assistant by the 21st Century COE Program 'Knowledge Information Infrastructure for Genome Science'.

References

1 Strong RW. Living-donor liver transplantation: an overview. *J Hepatobiliary Pancreat Surg* 2006; **13**:370–377.
2 Todo S, Furukawa H, Jin MB, Shimamura T. Living donor liver transplantation in adults: outcome in Japan. *Liver Transplant* 2000; **6 (Suppl 2)**:66–72.
3 Venkataramanan R, Swaminathan A, Prasad T, Jain A, Zuckerman S, Warty V, *et al.* Clinical pharmacokinetics of tacrolimus. *Clin Pharmacokinet* 1995; **29**:404–430.
4 Staatz CE, Tett SE. Clinical pharmacokinetics and pharmacodynamics of tacrolimus in solid organ transplantation. *Clin Pharmacokinet* 2004; **43**:623–653.
5 Masuda S, Inui K. An up-date review on individualized dosage adjustment of calcineurin inhibitors in organ transplant patients. *Pharmacol Ther* 2006; **112**:184–198.
6 Kahan BD, Keown P, Levy GA, Johnston A. Therapeutic drug monitoring of immunosuppressant drugs in clinical practice. *Clin Ther* 2002; **24**: 330–350.
7 Hebert MF. Contributions of hepatic and intestinal metabolism and P-glycoprotein to cyclosporine and tacrolimus oral drug delivery. *Adv Drug Deliv Rev* 1997; **27**:201–214.
8 Hashida T, Masuda S, Uemoto S, Saito H, Tanaka K, Inui K. Pharmacokinetic and prognostic significance of intestinal MDR1 expression in recipients of living-donor liver transplantation. *Clin Pharmacol Ther* 2001; **69**:308–316.
9 Masuda S, Goto M, Fukatsu S, Uesugi M, Ogura Y, Oike F, *et al.* Intestinal MDR1/ABCB1 level at surgery as a risk factor of acute cellular rejection in living-donor liver transplant patients. *Clin Pharmacol Ther* 2006; **79**: 90–102.
10 Goto M, Masuda S, Kiuchi T, Ogura Y, Oike F, Okuda M, *et al.* CYP3A5*1-carrying graft liver reduces the concentration/oral dose ratio of tacrolimus in recipients of living-donor liver transplantation. *Pharmacogenetics* 2004; **14**:471–478.
11 Uesugi M, Masuda S, Katsura T, Oike F, Takada Y, Inui K. Effect of intestinal CYP3A5 on postoperative tacrolimus trough levels in living-donor liver transplant recipients. *Pharmacogenet Genomics* 2006; **16**:119–127.
12 Sam WJ, Aw M, Quak SH, Lim SM, Charles BG, Chan SY, *et al.* Population pharmacokinetics of tacrolimus in Asian paediatric liver transplant patients. *Br J Clin Pharmacol* 2000; **50**:531–541.
13 García Sánchez MJ, Manzanares C, Santos-Buelga D, Blázquez A, Manzanares J, Urruzuno P, *et al.* Covariate effects on the apparent clearance

of tacrolimus in paediatric liver transplant patients undergoing conversion therapy. *Clin Pharmacokinet* 2001; **40**:63–71.
14 Staatz CE, Taylor PJ, Lynch SV, Willis C, Charles BG, Tett SE. Population pharmacokinetics of tacrolimus in children who receive cut-down or full liver transplants. *Transplantation* 2001; **72**:1056–1061.
15 Antignac M, Hulot JS, Boleslawski E, Hannoun L, Touitou Y, Farinotti R, *et al.* Population pharmacokinetics of tacrolimus in full liver transplant patients: modelling of the post-operative clearance. *Eur J Clin Pharmacol* 2005; **61**:409–416.
16 Zahir H, McLachlan AJ, Nelson A, McCaughan G, Gleeson M, Akhlaghi F. Population pharmacokinetic estimation of tacrolimus apparent clearance in adult liver transplant recipients. *Ther Drug Monit* 2005; **27**:422–430.
17 Lee JY, Hahn HJ, Son IJ, Suh KS, Yi NJ, Oh JM, *et al.* Factors affecting the apparent clearance of tacrolimus in Korean adult liver transplant recipients. *Pharmacotherapy* 2006; **26**:1069–1077.
18 Yasuhara M, Hashida T, Toraguchi M, Hashimoto Y, Kimura M, Inui K, *et al.* Pharmacokinetics and pharmacodynamics of FK 506 in pediatric patients receiving living-related donor liver transplantations. *Transplant Proc* 1995; **27**:1108–1110.
19 Fukatsu S, Yano I, Igarashi T, Hashida T, Takayanagi K, Saito H, *et al.* Population pharmacokinetics of tacrolimus in adult recipients receiving living-donor liver transplantation. *Eur J Clin Pharmacol* 2001; **57**: 479–484.
20 Fukudo M, Yano I, Masuda S, Goto M, Uesugi M, Katsura T, *et al.* Population pharmacokinetic and pharmacogenomic analysis of tacrolimus in pediatric living-donor liver transplant recipients. *Clin Pharmacol Ther* 2006; **80**: 331–345.
21 Kiuchi T, Kasahara M, Uryuhara K, Inomata Y, Uemoto S, Asonuma K, *et al.* Impact of graft size mismatching on graft prognosis in liver transplantation from living donors. *Transplantation* 1999; **67**:321–327.
22 Sugawara Y, Makuuchi M, Takayama T, Imamura H, Dowaki S, Mizuta K, *et al.* Small-for-size grafts in living-related liver transplantation. *J Am Coll Surg* 2001; **192**:510–513.
23 Mochizuki N, Matsumoto K, Ohno K, Shimamura T, Furukawa H, Todo S, *et al.* Effects of hepatic CYP3A4 activity on disposition of micafungin in liver transplant recipients with markedly small-for-size grafts. *Transplant Proc* 2006; **38**:3649–3650.
24 Kishino S, Ohno K, Shimamura T, Furukawa H, Todo S. A nomogram for predicting the optimal oral dosage of tacrolimus in liver transplant recipients with small-for-size grafts. *Clin Transplant* 2006; **20**:443–449.
25 Ojo AO, Held PJ, Port FK, Wolfe RA, Leichtman AB, Young EW, *et al.* Chronic renal failure after transplantation of a nonrenal organ. *N Engl J Med* 2003; **349**:931–940.
26 Hebert MF, Dowling AL, Gierwatowski C, Lin YS, Edwards KL, Davis CL, *et al.* Association between ABCB1 (multidrug resistance transporter) genotype and post-liver transplantation renal dysfunction in patients receiving calcineurin inhibitors. *Pharmocogenetics* 2003; **13**:661–674.
27 Hauser IA, Schaeffeler E, Gauer S, Scheuermann EH, Wegner B, Gossmann J, *et al.* ABCB1 genotype of the donor but not of the recipient is a major risk factor for cyclosporine-related nephrotoxicity after renal transplantation. *J Am Soc Nephrol* 2005; **16**:1501–1511.
28 Dai Y, Iwanaga K, Lin YS, Hebert MF, Davis CL, Huang W, *et al. In vitro* metabolism of cyclosporine A by human kidney CYP3A5. *Biochem Pharmacol* 2004; **68**:1889–1902.
29 Dai Y, Hebert MF, Isoherranen N, Davis CL, Marsh C, Shen DD, *et al.* Effect of CYP3A5 polymorphism on tacrolimus metabolic clearance *in vitro*. *Drug Metab Dispos* 2006; **34**:836–847.
30 Joy MS, Hogan SL, Thompson BD, Finn WF, Nickeleit V. Cytochrome P450 3A5 expression in the kidneys of patients with calcineurin inhibitor nephrotoxicity. *Nephrol Dial Transplant* 2007; **22**:1963–1968.
31 Cogill JL, Taylor PJ, Westley IS, Morris RG, Lynch SV, Johnson AG. Evaluation of the tacrolimus II microparticle enzyme immunoassay (MEIA II) in liver and renal transplant recipients. *Clin Chem* 1998; **44**:1942–1946.
32 Goto M, Masuda S, Saito H, Uemoto S, Kiuchi T, Tanaka K, *et al.* C3435T polymorphism in the MDR1 gene affects the enterocyte expression level of CYP3A4 rather than Pgp in recipients of living-donor liver transplantation. *Pharmacogenetics* 2002; **12**:451–457.
33 Chowbay B, Cumaraswamy S, Cheung YB, Zhou Q, Lee EJ. Genetic polymorphisms in MDR1 and CYP3A4 genes in Asians and the influence of MDR1 haplotypes on cyclosporin disposition in heart transplant recipients. *Pharmacogenetics* 2003; **13**:89–95.
34 Kuehl P, Zhang J, Lin Y, Lamba J, Assem M, Schuetz J, *et al.* Sequence diversity in CYP3A promoters and characterization of the genetic basis of polymorphic CYP3A5 expression. *Nat Genet* 2001; **27**:383–391.
35 Saeki M, Saito Y, Nakamura T, Murayama N, Kim SR, Ozawa S, *et al.* Single nucleotide polymorphisms and haplotype frequencies of CYP3A5 in a Japanese population. *Hum Mutat* 2003; **21**:653.
36 Beal SL, Boeckmann AJ, Sheiner LB. *NONMEM users guides*. San Francisco: NONMEM Project Group, University of California at San Francisco; 1992.
37 Kirchheiner J, Bauer S, Meineke I, Rohde W, Prang V, Meisel C, *et al.* Impact of CYP2C9 and CYP2C19 polymorphisms on tolbutamide kinetics and the insulin and glucose response in healthy volunteers. *Pharmacogenetics* 2002; **12**:101–109.
38 Yates CR, Zhang W, Song P, Li S, Gaber AO, Kotb M, *et al.* The effect of CYP3A5 and MDR1 polymorphic expression on cyclosporine oral disposition in renal transplant patients. *J Clin Pharmacol* 2003; **43**: 555–564.
39 Hesselink DA, van Gelder T, van Schaik RH, Balk AH, van der Heiden IP, van Dam T, *et al.* Population pharmacokinetics of cyclosporine in kidney and heart transplant recipients and the influence of ethnicity and genetic polymorphisms in the MDR-1, CYP3A4, and CYP3A5 genes. *Clin Pharmacol Ther* 2004; **76**:545–556.
40 Djebli N, Rousseau A, Hoizey G, Rerolle JP, Toupance O, Le Meur Y, *et al.* Sirolimus population pharmacokinetic/pharmacogenetic analysis and bayesian modelling in kidney transplant recipients. *Clin Pharmacokinet* 2006; **45**:1135–1148.
41 Aweeka FT, Benet LZ, Gambertoglio JG, Peter K, Okudaira N, Kinda J, *et al.* Comparative pharmacokinetics of orally (PO) and intravenously (IV) administered tacrolimus (FK506) in pre- and post-kidney transplant recipients. *Clin Pharmacol Ther* 1993; **53**:151.
42 Antignac M, Barrou B, Farinotti R, Lechat P, Urien S. Population pharmacokinetics and bioavailability of tacrolimus in kidney transplant patients. *Br J Clin Pharmacol* 2007; **64**:750–757.
43 Mouly SJ, Matheny C, Paine MF, Smith G, Lamba J, Lamba V, *et al.* Variation in oral clearance of saquinavir is predicted by CYP3A5*1 genotype but not by enterocyte content of cytochrome P450 3A5. *Clin Pharmacol Ther* 2005; **78**:605–618.
44 Yu S, Wu L, Jin J, Yan S, Jiamg G, Xie H, *et al.* Influence of CYP3A5 gene polymorphisms of donor rather than recipient to tacrolimus individual dose requirement in liver transplantation. *Transplantation* 2006; **81**:46–51.
45 Wei-lin W, Jing J, Shu-sen Z, Li-hua W, Ting-bo L, Song-feng Y, *et al.* Tacrolimus dose requirement in relation to donor and recipient ABCB1 and CYP3A5 gene polymorphisms in Chinese liver transplant patients. *Liver Transplant* 2006; **12**:775–780.
46 Venkatakrishnan K, von Moltke LL, Greenblatt DJ. Effects of the antifungal agents on oxidative drug metabolism: clinical relevance. *Clin Pharmacokinet* 2000; **38**:111–180.
47 Fukudo M, Yano I, Fukatsu S, Saito H, Uemoto S, Kiuchi T, *et al.* Forecasting of blood tacrolimus concentrations based on the Bayesian method in adult patients receiving living-donor liver transplantation. *Clin Pharmacokinet* 2003; **42**:1161–1178.
48 Kuypers DR, de Jonge H, Naesens M, Lerut E, Verbeke K, Vanrenterghem Y. CYP3A5 and CYP3A4 but not MDR1 single-nucleotide polymorphisms determine long-term tacrolimus disposition and drug-related nephrotoxicity in renal recipients. *Clin Pharmacol Ther* 2007; **82**:711–725.

Journal of Cellular Physiology

A Model for Diabetic Nephropathy: Advantages of the Inducible cAMP Early Repressor Transgenic Mouse Over the Streptozotocin-Induced Diabetic Mouse

AKARI INADA,[1,2] HIROSHI KANAMORI,[3] HIDENORI ARAI,[4]* TOMOYUKI AKASHI,[2] MAKOTO ARAKI,[3] GORDON C. WEIR,[2] AND ATSUSHI FUKATSU[3]

[1] *SSP Stem Cell Unit, Kyushu University Graduate School of Medicine, Fukuoka, Japan*

[2] *Islet Transplantation and Cell Biology, Joslin Diabetes Center, Boston, MA*

[3] *Department of Nephrology, Kyoto University Graduate School of Medicine, Kyoto, Japan*

[4] *Department of Geriatric Medicine, Kyoto University Graduate School of Medicine, Kyoto, Japan*

We have previously found progressive diabetic nephropathy in inducible cAMP early repressor (ICER Iγ) transgenic (Tg) mice. The ICER Iγ Tg mouse is an interesting model of sustained hyperglycemia due to its low production of insulin and insulin-producing β cells. Here in a longitudinal study we further analyzed diabetic nephropathy and structural and functional alterations in other organs, comparing our model with streptozotocin (STZ)-diabetic model mice. The high-dose STZ-diabetic model showed marked variation in blood glucose levels and severe toxicity of STZ in the liver and kidney. The low-dose STZ-diabetic model showed less toxicity, but the survival rate was very low. STZ-diabetic mice had much more variation of glomerular hypertrophy and sclerosis. Furthermore, non-specific toxicity of STZ or insulin injections to maintain optimal blood glucose levels might have another effect upon the diabetic renal changes. In contrast, ICER Iγ Tg mice exhibited a stable and progressive phenotype of diabetic kidney disease solely due to chronic hyperglycemia without other modulating factors. Thus, ICER Iγ Tg mouse has advantages for examining diabetic renal disease, and offers unique and very different perspectives compared to STZ model.

J. Cell. Physiol. 215: 383–391, 2008.

Biomedical experiments in mice provide significant advantages for studying mammalian diseases since inbred mice have a uniform genetic background. To investigate the pathogenesis of diabetic nephropathy, appropriate animal models are required. Although numerous animal models have been established in rodents (Breyer et al., 2005), these diabetic animals develop limited or only mild kidney disease that resembles human diabetic nephropathy (Tochino, 1987; Williamson et al., 1987; Doi et al., 1990; Janssen et al., 2003), and no single animal model that develops renal changes identical to those seen in humans has been developed (Velasquez et al., 1990).

So far the streptozotocin (STZ)-induced diabetic mouse model is commonly used. STZ-induced DNA damage leads to reduction of the cellular ATP content and then death of pancreatic β cells (Szkudelski, 2001). Low-dose STZ elicits non-specific islet inflammation with infiltrating mononuclear cells (Like and Rossini, 1976; Like et al., 1978). High-dose single injections of STZ cause β-cell necrosis within 2–4 h (Junod et al., 1967) with rapid clearance of STZ (Schein et al., 1973). Because neonatal STZ-treatment has oncogenic effects on liver, kidney, and pancreas (Iwase et al., 1989), adult animals are used for induction of diabetes. However, there are several problems in this model: (I) STZ is harmful and carcinogenic for animals (Like and Rossini, 1976; Like et al., 1978), and induces toxicity in multiple organs (Nukatsuka et al., 1990; Sotnikova et al., 1999; Wang et al., 2000; Imaeda et al., 2002; Koulmanda et al., 2003; Brondum et al., 2005). STZ is taken up by a glucose transporter into renal proximal tubular cells to induce tubular alterations (Sadoff, 1970; Tay et al., 2005). High-dose STZ directly damages and alters the renal function during the first week after STZ injection. In addition, STZ affects not only renal excretion of electrolytes and protein, but also renal microcirculation and oxygen metabolism (Palm et al., 2004). Therefore, the renal damage in STZ mice is induced not only by hyperglycemia but by

Contract grant sponsor: Scientific Research, Ministry of Education, Culture, Sports, Science and Technology;
Contract grant number: 19890150.
Contract grant sponsor: Creative Scientific Research, Ministry of Education, Culture, Sports, Science and Technology;
Contract grant number: NP10NPO201.
Contract grant sponsor: Japan Society for the Promotion of Science;
Contract grant number: JSPS-RFTF97100201.
Contract grant sponsor: Japan Diabetes Foundation.
Contract grant sponsor: Mochida Memorial foundation.

Akari Inada's present address is SSP Stem Cell Unit, Kyushu University Graduate School of Medicine, 3-1-1 Maidashi, Higashi-ku, Fukuoka 812-8582, Japan.

*Correspondence to: Hidenori Arai, Department of Geriatric Medicine, Kyoto University Graduate School of Medicine, 54 Kawahara-cho, Shogoin, Sakyo-ku, Kyoto 606-8507, Japan.
E-mail: harai@kuhp.kyoto-u.ac.jp

Received 27 August 2007; Accepted 11 September 2007

DOI: 10.1002/jcp.21316

STZ itself (Churchill et al., 1993; Lee et al., 1974). (II) To maintain optimal blood glucose levels for survival, daily insulin injections are often required, and it is difficult to maintain optimal glucose levels. Insulin might have additional effects on diabetic renal changes. (III) STZ is not sufficient for a useful model of progressive renal disease. STZ mice show mesangial expansion, but they show glomerulosclerosis only in limited backgrounds (Breyer et al., 2005, 2006). STZ plus subtotal nephrectomy (Yokozawa et al., 2001) or STZ plus high protein diet (Zatz et al., 1985) has been used to accelerate the process. (IV) In STZ mice, much more variation of renal lesions is observed, which makes it difficult to evaluate the nephropathy correctly and requires a large number of mice for proper statistical analysis of the renal disease.

We previously developed a severe diabetic mouse model, inducible cAMP early repressor (ICER Iγ) transgenic (Tg) mice (Inada et al., 2004). ICER Iγ is a transcriptional repressor transcribed from an alternative intronic promoter of the *CREM* gene and consists of only a DNA-binding domain (Foulkes et al., 1991; Inada et al., 1998). ICER Iγ competes with transcriptional activators for binding to the DNA, and strongly represses insulin (Inada et al., 1999) and cyclin A (Inada et al., 2005a) gene transcription. In this mouse, ICER Iγ is overexpressed only in pancreatic β cells, not in other organs (Inada et al., 2004). The suppression of insulin synthesis and β cell proliferation results in severe diabetes as early as 2 weeks of age (Inada et al., 2004). Hyperglycemia is sustained by 40 weeks of age, but mice show an excellent survival rate without insulin therapy (Inada et al., 2004). In this model, we have found that the diabetic renal change starts with glomerular hypertrophy, followed by glomerular basement membrane (GBM) thickening and development of sclerotic lesions, thus mimicking the progression of human diabetic nephropathy (Inada et al., 2005b).

Here, in a longitudinal study, we further analyzed diabetic nephropathy and functional and morphological alterations of other organs (liver and pancreas), comparing our model with STZ mice. Our model offers a unique and very different perspective of diabetic nephropathy compared to STZ-diabetic mice.

Materials and Methods

Generation of ICER Iγ Tg mice

ICER Iγ transgenic (ICER Tg) mice were made as described previously (Inada et al., 2004). Their background strain is C57BL/6J (Japan SLC, Inc., Hamamatsu, Shizuoka, Japan). Three transgenic lines (Tg 7, Tg 12, Tg 23) were obtained from 62 founder mice. Copy numbers of the transgene in founder mice were 4, 4, and 6, respectively, determined by Southern blot analysis. Tg mice were identified by PCR analysis of tail DNA. In all experiments, non-transgenic littermates (wild type, WT) were used as controls. Mice were housed in microisolator cages in a temperature-controlled room at 24 ± 2°C and at 50 ± 10% relative humidity under 12-h light/dark cycle. Standard rodent diet (CE-2; CLEA Japan, Inc., Tokyo, Japan) and water were supplied ad libitum. All mice were handled in accordance with the Guidelines for Animal Experiments of Kyoto University. The data presented here are from F2 to F4 males only of line Tg 23.

STZ-induced diabetic model mouse

Weight-matched 8-week-old male mice (C57BL/6J) were treated with STZ (Sigma Chemical Co., St. Louis, MO) or sterile citrate buffer (pH 4.5) alone, according to the animal models of diabetic complications consortium (AMDCC) protocol. STZ was freshly dissolved in sterile citrate buffer (pH 4.5) and injected intraperitoneally into mice (50, 150, or 200 mg/kg). Mice treated with 50 mg/kg of STZ (STZ-50) were fasted for 4-h prior to STZ induction, and were given one injection for 5 days consecutively. Mice treated with 150 or 200 mg/kg of STZ (STZ-150 or -200) were given a single i.p. injection of STZ. Only mice with blood glucose concentrations greater than 400 mg/dl in the fed state were used as diabetic in the experiments for each group.

Histological study

ICER Tg, STZ and control (N = 6 for each group) mouse kidney, pancreases, and livers were fixed in methyl Carnoy's solution or 10% buffered formalin, embedded in paraffin, and cut in serial sections (2 μm). Kidney sections were stained with periodic acid-Schiff (PAS) and periodic acid-methenamine silver (PASM). Liver and pancreas sections were stained with hematoxylin and eosin (H&E) using standard histological procedures.

Measurements of glomerular surface area and PASM-positive area. PASM-positive area and glomerular surface area were measured in PASM stained sections using Image-Pro Plus (Media Cybernetics, Silver Spring, MD). For each mouse, 50 glomeruli were analyzed. PASM-positive area fraction was calculated as the ratio of PASM-positive area to glomerular surface area (Nagai et al., 2003).

Immunohistochemistry

Mouse pancreases were fixed in 10% buffered formalin, embedded in paraffin, and cut in serial sections (2 μm). For immunohistochemistry, primary antibodies, anti-insulin (1:500; DAKO), anti-ICER (anti-serum α-CREM S4; 1:500; kindly provided J. F. Habener, Maassachusetts General Hospital, Howard Hughes Medical Institute), and anti-glucagon (1:3,000; Linco Reasearch, Inc., St. Charles, MO) were used. Primary antibody was detected by immunofluorescence labeling with FITC-conjugated or Texas red-conjugated secondary antibodies or by imunoperoxidase with biotin-labeled secondary antibody. Staining was visualized with diaminobenzidine.

Measurements of serum variables

Blood glucose levels were determined by an enzyme-electrode method using GLUTEST (Sanwa Kagaku, Nagoya, Japan) on whole blood taken from the tail vein. For other parameters, blood was withdrawn from the heart immediately before isolation of the kidney under pentobarbital anesthesia. Creatinine was measured by HPLC. Total cholesterol was measured by enzymatic assays (Wako Pure Chemical Industries Ltd., Kyoto, Japan). Albumin was measured by BCG method (SRL, Inc., Tokyo, Japan).

Measurements of urinary variables

The urinary parameters measured were albumin and creatinine. They were measured at 8–40 weeks of age in 24-h urine collection samples from mice housed in individual metabolic cages (N = 6 in each group). During the urine collection, mice were allowed free access to food and water. Albumin concentration was assayed using the Albuwell kit (Exocell, Inc., Philadelphia, PA). Creatinine was measured by HPLC as described above. Body-weight adjusted creatinine clearance (Ccr) was calculated by the following equation: Ccr = urine creatinine (mg/dl) × urine volume (μl/min)/serum creatinine (mg/dl)/body weight (g) (Nagasao et al., 2005).

Data analysis

Data are presented as mean ± SD. Comparison among each group was performed by one-way analysis of variance (ANOVA) followed by Neuman–Keuls test to evaluate statistical significance between two groups. For multiple comparison and changes in blood glucose levels, repeated measure ANOVA, Kruskal–Wallis test, and post hoc Bonferroni/Dunn test were used. A *P*-value less than 0.05 was considered statistically significant.

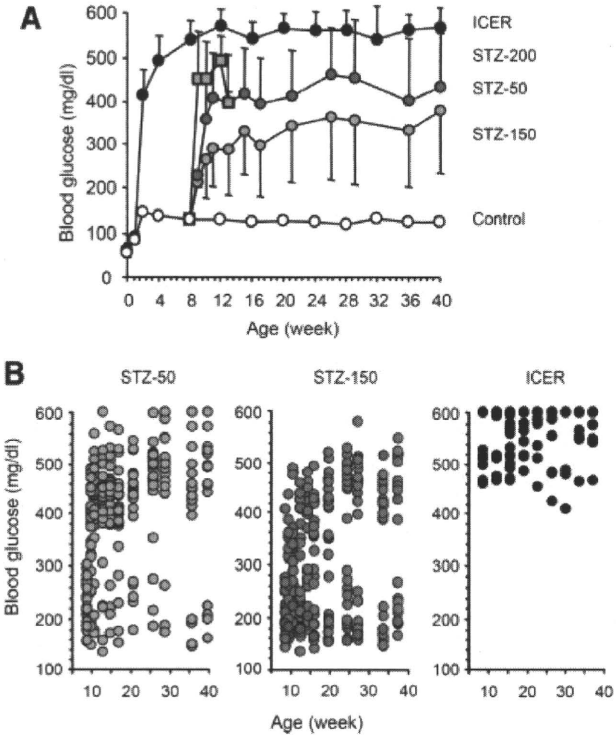

Fig. 1. ICER Tg mice exhibited sustainable hyperglycemia. A: Fed blood glucose levels at indicated weeks. The three dose of STZ (50 or 150 or 200 mg/kg) were injected intraperitoneally into male mice at 8 weeks of age. Fed blood glucose levels of STZ-200 mice (light-gray square) elevated very fast, and they died within 4–8 weeks of injection. Increase of fed blood glucose levels of STZ-50 mice (dark-gray circle) and STZ-150 mice (light-gray circle) were more gradual but unstable. In ICER Tg mice (black circle) severe hyperglycemia was sustained. Results are expressed as mean ± SD. B: In STZ-diabetic mice, there is a marked variation of fed blood glucose levels. N = 24 for each STZ-diabetic group, N = 14 for ICER Tg mice. Each circle represents an animal, but some circles represent 5–9 animals since they had same blood glucose levels (black circle in ICER Tg mice).

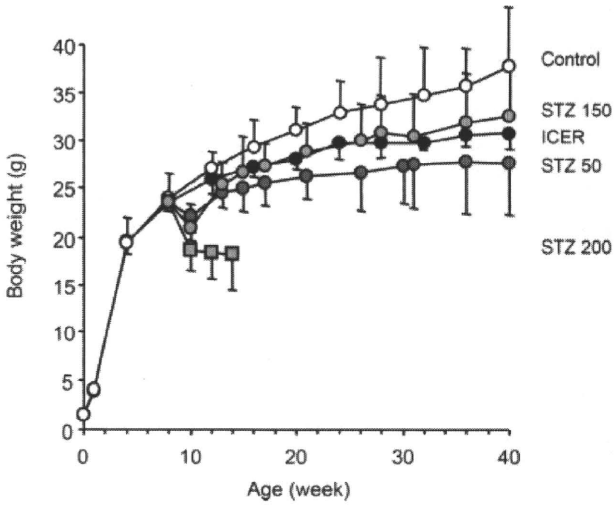

Fig. 2. Body weight of male mice. The growth curve of male mice from day 0 to 40 weeks of age is shown. STZ-200 mice (light-gray square) lost body weight and died soon. Results are expressed as mean ± SD. N = 24 for each STZ-diabetic group, N = 14 for ICER Tg mice.

Results

ICER Tg mice exhibit sustained hyperglycemia

In ICER Tg mice, blood glucose levels were normal at birth, but became markedly increased by 2 weeks of age, and severe hyperglycemia was sustained at least until 40 weeks of age (Fig. 1A). These mice survived well without insulin therapy, and had no obesity or severe emaciation. In STZ-50 and STZ-150 mice, following injection of STZ, blood glucose levels became gradually hyperglycemic within 3 weeks, and increased until 26 weeks of age. In addition, there was a marked variation of fed blood glucose levels in STZ mice (Fig. 1B). STZ-200 mice developed severe diabetes soon after the STZ injection (Fig. 1A), with a sharp drop in body weight (Fig. 2), which led to death within 4–8 weeks of injection.

In ICER Tg mice, body weight was similar to that of controls until 8 weeks of age, but they failed to gain weight thereafter (Fig. 2). STZ-150 mice showed a similar body weight change to ICER Tg mice, but started to gain weight after 30 weeks of age. Body weight of STZ-50 mice was lower than that of ICER Tg mice at all time points during the study, with only a slight increase after STZ injection.

Eleven out of 24 diabetic STZ-50 mice survived for the entire 40 weeks. Soon after 40 weeks three more mice died. In contrast, the survival rate of ICER Tg mice was excellent; 12 of 14 ICER Tg mice survived.

Islet morphology

STZ causes preferential death of pancreatic β cells by its uptake in these cells via GLUT-2 glucose transporter. Because there are few insulin-positive cells left in islets, pancreatic sections from 40-week old mice were immunostained for glucagon. In controls, the typical islet morphology of a mantle of glucagon-positive cells (brown) was seen (Fig. 3A, left). In contrast, in STZ-150 mice, the islets appeared severely disorganized with an increased proportion of glucagon-positive cells (Fig. 3A, middle). In STZ-50 mice, there was a marked variation in islet size and the number of β cells in the islet as shown in Figure 3B. The islet morphology in STZ mice was similar to that of ICER Tg mice. In ICER Tg mice, insulin-positive cells (green) are reduced due to ICER expression (red) (Fig. 3C), so the islets appear severely disorganized with a significantly increased proportion of glucagon-positive cells (Fig. 3A, right). Thus, serum insulin levels were extremely low (12 weeks, line Tg23 male Tg mice vs. control male mice, 278 ± 111 vs. 1,350 ± 195 pg/ml, $P < 0.001$).

Liver toxicity of STZ

The liver toxicity was examined by measuring organ weights and serum aspartate aminotransfase (AST) and alanine aminotransfase (ALT) levels. There was no significant difference in liver weight (Fig. 4A), but liver weight/body weight in STZ-diabetic mice was higher than that in ICER Tg mice at 40 weeks of age (Fig. 4B). ICER liver weight/body weight was probably a little high due to modest body weight decrease from controls. The ratio of AST/ ALT was significantly increased in STZ-diabetic mice group (Fig. 4C). The liver section showed severe hepatic steatosis in STZ-diabetic mice (Fig. 5).

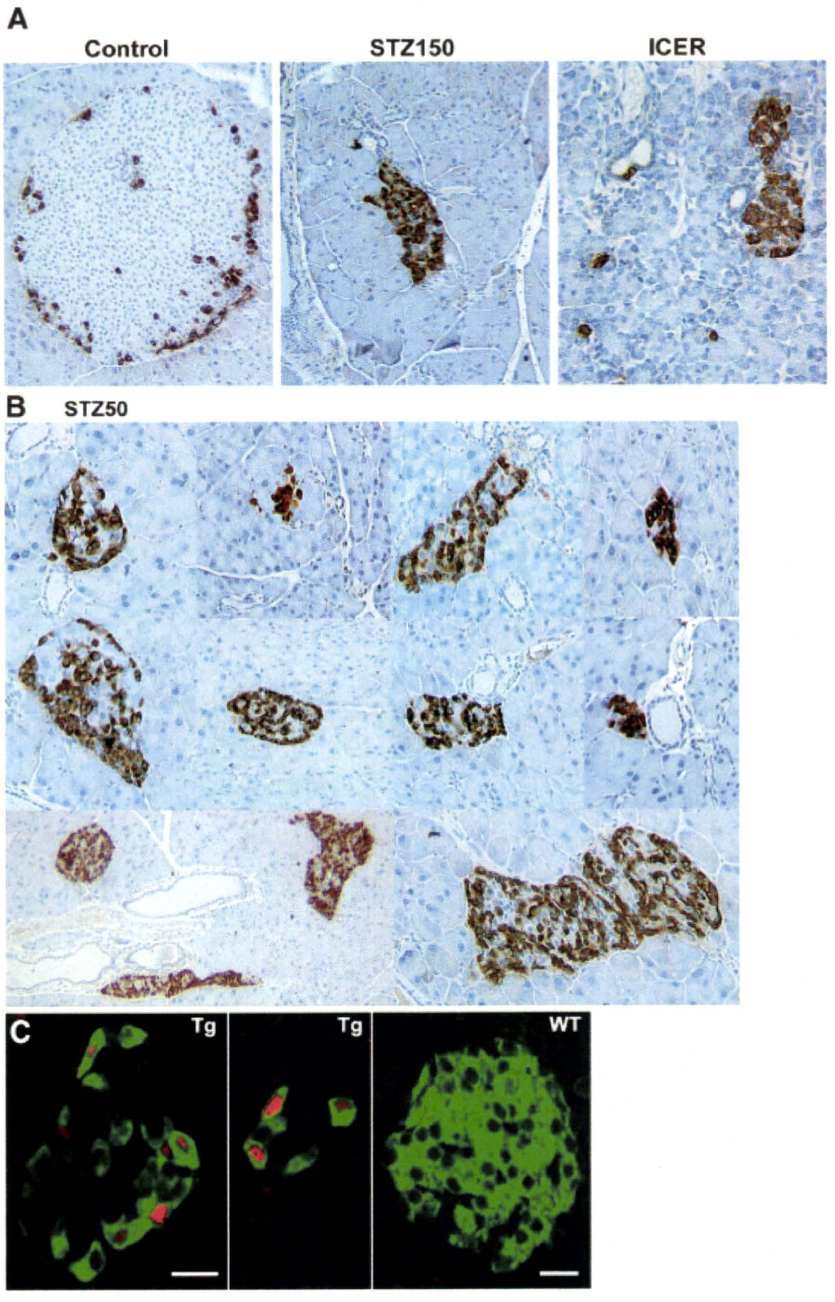

Fig. 3. Islet morphology. Glucagon staining of pancreatic sections of 40 week-old-mice. A: In STZ-150 mice and ICER Tg mice, islets appear severely disorganized with a significantly increased proportion of glucagon-positive (brown) cells. B: In STZ-50 mice there is a variation in the size as shown by the glucagon staining. The non-stained cells present as aggregating in the middle of the islets are assumed to be β cells. Magnification, 200× (A–D) and 100× (D, left low panel only). C: Reduced insulin synthesis and β-cell numbers in a representative islet. Dual staining of pancreatic sections with anti-insulin (green) and anti-ICER (red) antibody was analyzed by confocal microscopy.

Diabetic nephropathy

Glomerular hypertrophy and subsequent glomerulosclerosis are the characteristic histological findings lesions in diabetic nephropathy. To analyze the hypertrophy and glomerulosclerosis, we measured glomerular surface area and PASM-positive areas. Renal glomerular sclerotic lesions seen in STZ nice are variable and they were milder (Fig. 6A,B), whereas lesions in Tg mice were more severe and constant (Fig. 6C). There was a significant difference in PASM-positive areas between STZ-150 mice and ICER Tg mice ($P = 0.014$) (Fig. 6D).

Renal functional measurement

Clearance studies are some of the most valuable means of determining the stage of nephropathy, with Ccr, a reliable test to measure GFR. In both STZ-diabetic mice and ICER Tg mice, Ccr was significantly higher at 40 weeks of age than in controls

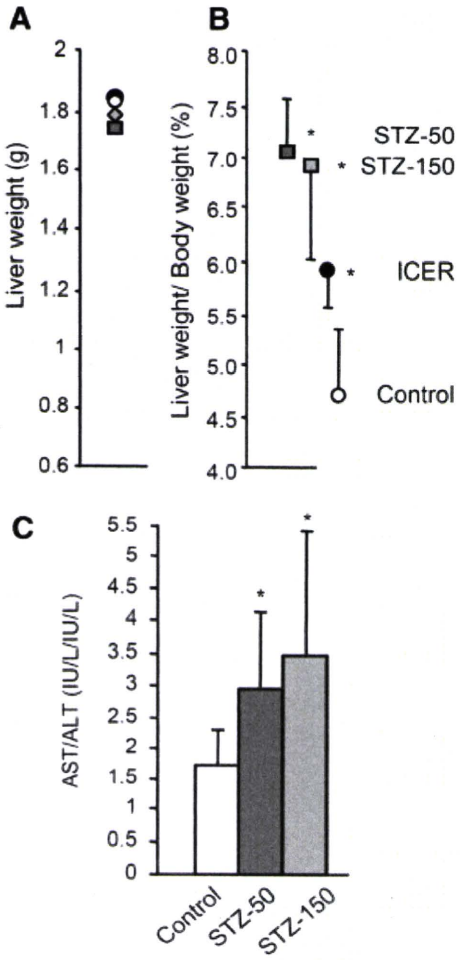

Fig. 4. The damage of the liver in STZ-diabetic mice. A: Liver weight. B: Liver weight/ body weight of STZ-diabetic mice at 40 weeks of age was elevated, since they had lower body weight. C: The AST/ALT ratio was significantly increased in STZ-diabetic mice. Results are expressed as mean ± SD. N = 6 for each group.

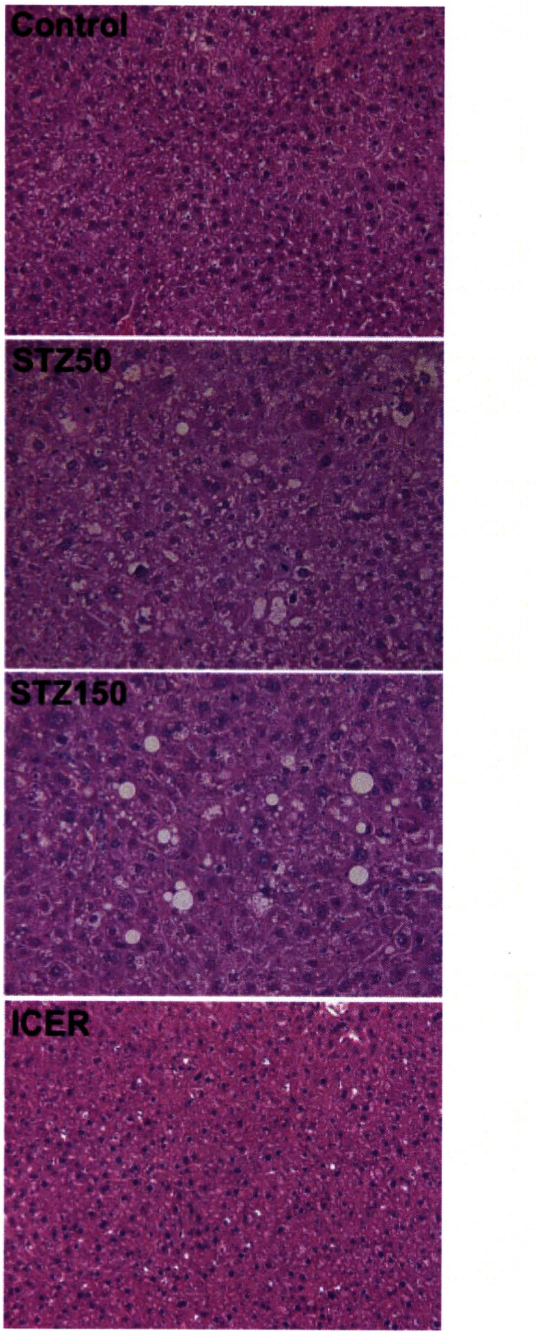

Fig. 5. Liver morphology. Hematoxylin and eosin (H&E) staining at 40-week-old mice. STZ-150 mice show marked steatosis and cholestasis. Magnification, 200×.

(Fig. 7A,B). In ICER Tg mice, the peak of Ccr was at 20 weeks of age, and then decreased toward 40 weeks of age. There was no significant difference in serum creatinine at 40 weeks of age (Fig. 7C). We also examined kidney weights. Renal hypertrophy was expressed as the ratio of the total kidney weight (the combined weight of the two kidneys) to body weight. In ICER Tg mice, the kidney weight increased with age (Fig. 7D), and renal hypertrophy was also prominent (Fig. 7E), which started at 8 weeks of age. In contrast, in STZ mice the kidney weight was not increased and showed no significant difference from controls (Fig. 7D). Renal hypertrophy was seen in STZ mice, but less than that in ICER Tg mice at 40 weeks of age (Fig. 7E). The urinary albumin excretion rates in both ICER Tg mice and STZ mice were higher at 40 weeks of age than in control mice (Fig. 8A). At the same time, serum albumin was significantly lower (Fig. 8B) and urine volume and total cholesterol were higher in both ICER Tg mice and STZ-diabetic mice than in control mice (Fig. 8C,D).

Discussion

In this longitudinal study, we assessed diabetic nephropathy and structural and functional alterations in organs in ICER Tg mouse and compared them with corresponding changes in STZ-induced diabetic mice. To assess the toxicity of this diabetologenic agent to organs, we used high- and low-dose STZ according to the AMCC protocol.

First, we assessed the pancreatic morphology in these models. Although single injections of high-dose STZ show marked variation in blood glucose levels, and are toxic to other organs (Sotnikova et al., 1999; Koulmanda et al., 2003), we consistently observed irreversible and complete destruction of β cells in diabetic STZ-150 mice. On the other hand, low-dose

STZ with multiple injections damages β cells more slowly within 12 h of STZ-treatment (Nagasao et al., 2005) with lower toxicity to other organs (Koulmanda et al., 2003), but it causes a variation in the degree of β-cell death, this leaving some residual β cells in STZ-50 mice. Susceptibility to the low-dose STZ appeared to be somewhat different in each animal, and more than half of the mice could not survive for the entire 40 weeks. Thus, destroying β cells by giving a chemical compound seems to cause varying levels of β-cell death, blood glucose levels, and survival. Since blood glucose levels and the diabetic period greatly affect the development of diabetic nephropathy, it was hard to produce stable renal changes in a sufficient number of STZ mice in this longitudinal study.

In contrast, in ICER Tg mice, both insulin synthesis and β-cell proliferation are suppressed genetically by overexpression of ICER Iγ. Insulin synthesis is substantially repressed at the transcriptional level from the fetal period. Normally the burst of β-cell replication after birth is important to expand β-cell population to produce enough insulin (Bonner-Weir, 2000). In ICER Tg mice, however, β-cell proliferation is limited through reduced cyclin A expression, which is required for normal cell cycle progression. Limitation of β-cell proliferation reduces not only β-cell number within islets but also insulin production. Therefore, ICER Tg mice uniformly lose β cells with time but retain a small number, which accounts for the maintenance of stable hyperglycemia.

In STZ-injected animals, complications include toxicity of aorta (Sotnikova et al., 1999), arteries (Brondum et al., 2005), liver, and kidney (Koulmanda et al., 2003); DNA damage in these tissues is well studied (Wang et al., 2000; Imaeda et al., 2000). In the STZ liver and kidney, DNA synthesis and tissue repair responses are delayed (Wang et al., 2000), oxygen consumption of mitochondria is decreased in a time- and dose-dependent manner (Nukatsuka et al., 1990), which increases necrosis from 12 h onward and progresses (Wang et al., 2000). Although DNA damage in the liver and kidney recovers slowly with time (Imaeda et al., 2002), we still found injury in these organs in STZ mice at 40 weeks of age. Elevated AST/ALT ratio and severe hepatic steatosis showed that liver was both functionally and morphologically damaged.

It is well known that hyperglycemia induces formation of reactive oxygen species (ROS), and that ROS, transforming growth factor-β1 (TGF-β1), and hypertension enhance the progression of diabetic nephropathy (Palm, 2006; Tesch and Nikolic-Paterson, 2006; Lee et al., 2007; Tojo et al., 2007). It has been also reported that the oxidative stress is mainly associated with hypertension in diabetic renal injury, and not associated as strongly with hyperglycemia (Tomohiro et al., 2007). We have measured systolic blood pressure (SBP) using tail-cuff method at 20 weeks of age. SBP in the ICER Tg mouse group was slightly higher than that in WT mouse group (Tg vs. WT, 113.1 ± 0.8 vs. 96.4 ± 0.8 mmHg, $P < 0.01$). Therefore, in ICER Tg mice it is possible that ROS are produced by sustained hyperglycemia, and oxidative stress could be associated with hypertension. Since it seems complex, further study is needed to find a factor playing a major role in progression of diabetic nephropathy in this model.

There are four advantages of ICER Tg mice compared to STZ mice: (1) ICER Tg mice stably develop hyperglycemia and renal changes. Hyperglycemia develops at about 2 weeks of age and continues throughout life, and these mice show excellent survival. Since each mouse has almost identical diabetic renal

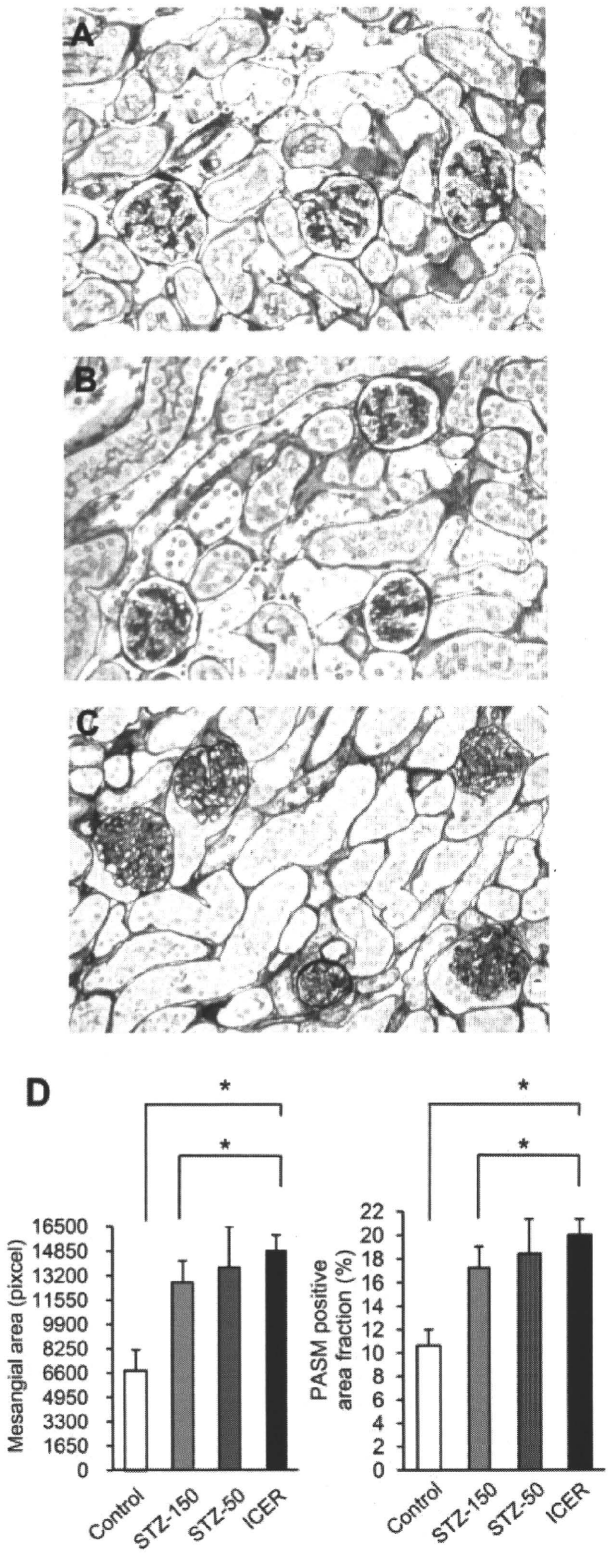

Fig. 6. Diabetic nephropathy. A–C: Representative glomeruli from 40-week-old mice. Renal glomerular sclerotic lesions seen in STZ nice are variable and they were milder (A,B), whereas lesions in Tg mice were more severe and constant (C). D: PASM-positive area was measured by image-Pro Plus in 50 glomeruli for each mouse. PASM-positive area fraction was calculated by the ratio of PASM-positive area to total glomerular surface area. Data are mean ± SD. N = 6 per each group. Kidney sections were stained with PASM. Magnification, 200×.

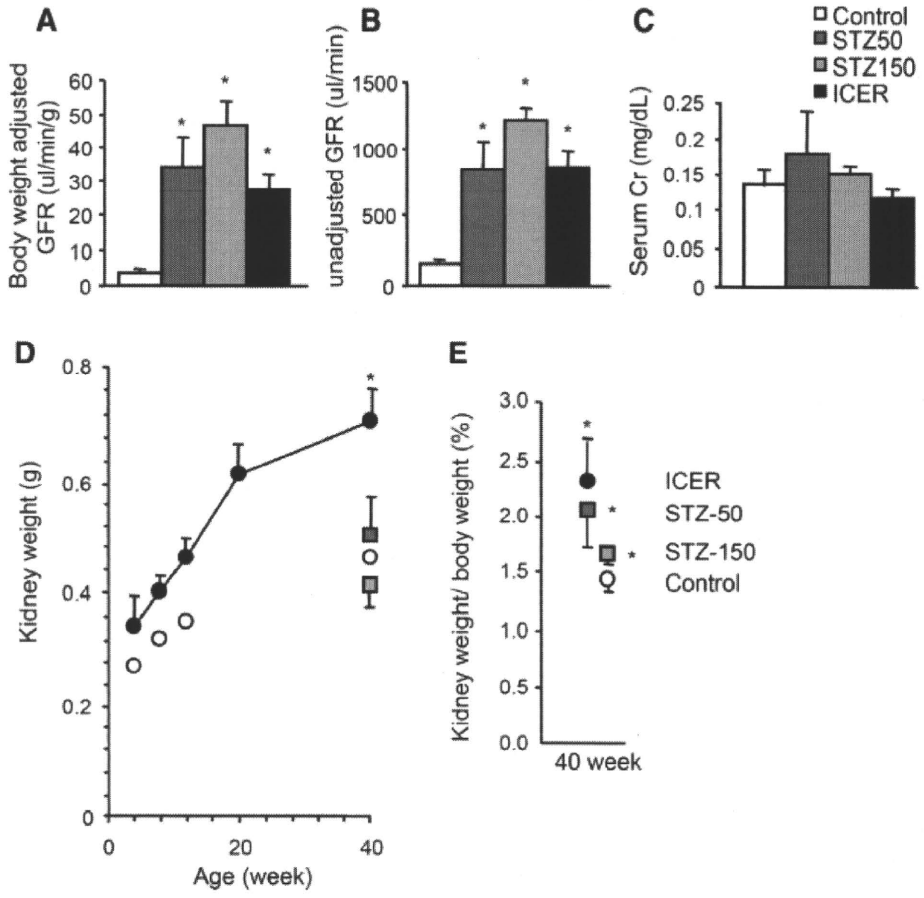

Fig. 7. Hemodynamic change in STZ-diabetic and ICER Tg mice. A,B: The glomerular filtration rate (GFR) was calculated as described in Materials and Methods Section. C: Serum creatinine was measured by HPLC. D: Kidney weight curve in ICER Tg mice (black circle) from 4 to 40 weeks of age and kidney weight in STZ-diabetic mice at 40 weeks of age. Control mice (white circle), STZ-50 mice (dark-gray square), STZ-150 (light-gray square). E: Kidney weight/body weight at 40 weeks of age. All Data are mean ± SD. *$P < 0.05$. N = 6 per each group.

disease, analysis of histological and functional changes is easier. However, in STZ-diabetic mouse the development of hyperglycemia is not consistent. Only half develop severe diabetes in 3 weeks after high-dose STZ injection. Moreover, in low-dose STZ mice, the survive rate is very low. Therefore, in STZ mice, because much more variation of renal lesions is observed, it is difficult to evaluate the nephropathy correctly and a larger number of mice are required to examine the renal disease statistically. (2) ICER Tg mouse stably expresses major clinical and pathological features of human diabetic nephropathy. The process of diabetic renal changes in this model is similar to those in humans: At 8 weeks, GFR was already increased and glomerular hypertrophy was prominent (the earliest stage of human diabetic nephropathy). At 20 weeks, a peak in GFR and an increase in the urinary albumin excretion rate were seen (the early to middle stage of human diabetic nephropathy). At 40 weeks, messangial matrix expansion, diffuse glomerular sclerotic lesions and GBM thickening, declined GFR, increased urinary albumin excretion rate, lower serum albumin, and higher serum total cholesterol levels were observed (the advanced stage of human diabetic nephropathy) (Inada et al., 2005b). However, other characteristic diabetic lesion, such as nodular sclerotic lesions or exudative lesions seen in human diabetic nephropathy were not observed in this model. In contrast, STZ mice show mesangial expansion with time and glomerulosclerosis only in limited backgrounds (Breyer et al., 2005). (3) Mechanism of renal functional changes in ICER Tg mouse is different from those of STZ mice. Since ICER is expressed only in pancreatic β cells but not in other organs (Inada et al., 2004), it is feasible to investigate the specific effect of hyperglycemia in this model. However, in STZ-diabetic model the direct toxic effect of STZ cannot be excluded, as shown in the hepatic and renal changes. STZ is taken up by a glucose transporter into renal proximal tubular cells and generates nitric oxide (NO), which is likely to account for the non-specific cytotoxicity resulting in acute kidney tubular damage (Sadoff, 1970; Kwon et al., 1994; Tay et al., 2005). Thus, the renal damage on STZ-diabetic mice is due to complex separate toxic effects of STZ and hyperglycemia (Lee et al., 1974; Churchill et al., 1993). (4) The ICER model is easy to produce: they can easily be crossed with normal C57BL/6 mice, and identified by the blood glucose measurements. Once ICER Tg mice develop diabetes by 2–3 weeks of age, they can survive without insulin injections. Since it is hard for low-dose STZ-diabetic mice to survive with uncontrolled blood glucose for a long time, we are often obligated to control blood glucose levels by daily insulin injections and even with this optimal glucose control is difficult to achieve. In addition, insulin might have other effect upon the diabetic renal changes.

In summary, we demonstrated an advantage of our diabetic mouse model compared with STZ mice. ICER Tg mice thus provide an excellent experimental diabetes model for studying

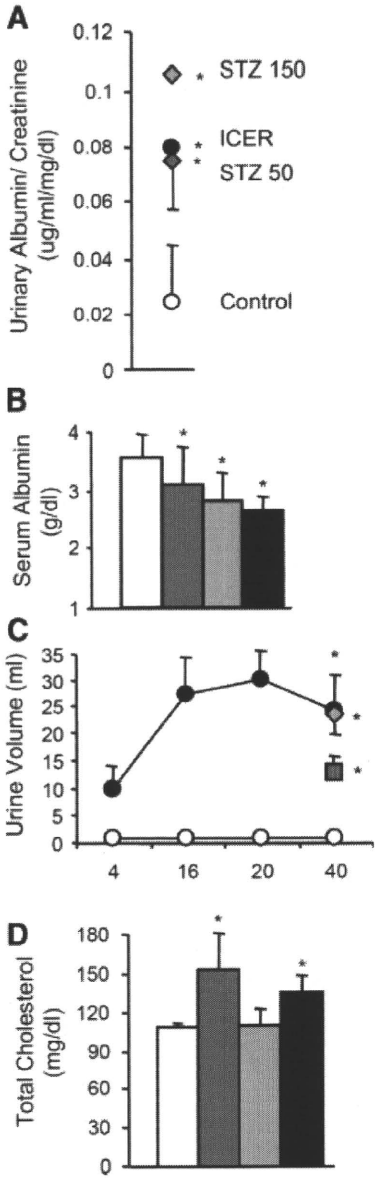

Fig. 8. Renal functional change in STZ-diabetic and ICER Tg mice. A: Urinary albumin excretion rate, (C) urine volume curve, and (D) total serum cholesterol was increased at 40 weeks of age. B: Serum albumin was low: from left, control (white), STZ-50 (dark-gray), STZ-150 (light-gray), ICER Tg mice (black). (C) STZ-150 (light-gray diamond), STZ-50 mice (dark-gray square). All Data are mean ± SD. *$P < 0.05$. N = 6 per each group.

the pathogenesis and to assessing the treatment of diabetic nephropathy and other complications, replacing STZ-induced diabetes animals.

Acknowledgments

We thank Hideo Uchiyama (Taigenkai Hospital) for technical assistance. This study was supported by Scientific Research (19890150) and Creative Scientific Research (NP10NPO201) from The Ministry of Education, Culture, Sports, Science and Technology (MEXT), "Research for the Future Program" from the Japan Society for the Promotion of Science (JSPS-RFTF97I00201), Japan Diabetes Foundation, and Mochida Memorial Foundation.

Literature Cited

Bonner-Weir S. 2000. Islet growth and development in the adult. J Mol Endocrinol 24:297–302.
Breyer MD, Bottinger E, Brosius FC III, Coffman TM, Harris RC, Heilig CW, Sharma K. 2005. AMDCC: Mouse models of diabetic nephropathy. J Am Soc Nephrol 16:27–45.
Breyer MD, Zhonghua Qi, Tchekneva E. 2006. Diabetic nephropathy: leveraging mouse genetics. Curr Opin Nephrol Hypertens 15:227–232.
Brondum E, Nilsson H, Aalkjaer C. 2005. Functional abnormalities in isolated arteries from Goto-Kakizaki and streptozotocin-treated diabetic rat models. Horm Metab Res 1:56–60.
Churchill P, Churchill M, Bidani A, Dunbar J, Jr. 1993. Streptozotocin-induced renal hemodynamic changes in isogenic Lewis rats: A kidney transplant study. Am J Physiol 264:F100–F105.
Doi T, Hattori M, Agodoa LY, Sato T, Yoshida H, Striker LJ, Striker GE. 1990. Glomerular lesions in nonobese diabetic mouse: Before and after the onset of hyperglycemia. Lab Invest 63:204–212.
Foulkes NS, Borrelli E, Sassone-Corsi P. 1991. CREM gene: Use of alternative DNA-binding domains generates multiple antagonists of cAMP-induced transcription. Cell 64:739–749.
Imaeda A, Kaneko T, Aoki T, Kondo Y, Nagase H. 2002. DNA damage and the effect of antioxidants in streptozotocin-treated mice. Food Chem Toxicol 40:979–987.
Inada A, Yamada Y, Someya Y, Kubota A, Yasuda K, Ihara Y, Kagimoto S, Kuroe A, Tsuda K, Seino Y. 1998. Transcriptional repressors are increased in pancreatic islets of type 2 diabetic rats. Biochem Biophys Res Commun 253:712–718.
Inada A, Someya Y, Yamada Y, Ihara Y, Kubota A, Ban N, Watanabe R, Tsuda K, Seino Y. 1999. The cyclic AMP response element modulator family regulates the insulin gene transcription by interacting with transcription factor IID. J Biol Chem 274:21095–21103.
Inada A, Hamamoto Y, Tsuura Y, Miyazaki J, Toyokuni S, Ihara Y, Nagai K, Yamada Y, Bonner-Weir S, Seino Y. 2004. Overexpression of inducible cyclic AMP early repressor inhibits transactivation of genes and cell proliferation in pancreatic β cells. Mol Cell Biol 24:2831–2841.
Inada A, Weir GC, Bonner-Weir S. 2005a. Induced ICER Iγ down-regulates cyclin A expression and cell proliferation in insulin-producing β cells. Biochem Biophys Res Commun 329:925–929.
Inada A, Nagai K, Arai H, Miyazaki J, Nomura K, Kanamori H, Toyokuni S, Yamada Y, Bonner-Weir S, Weir GC, Fukatsu A, Seino Y. 2005b. Establishment of a diabetic mouse model with progressive diabetic nephropathy. Am J Pathol 167:327–336.
Iwase M, Nunoi K, Sadoshima S, Kikuchi M, Fujishima M. 1989. Liver, kidney and islet cell tumors in spontaneously hypertensive and normotensive rats treated neonatally with streptozotocin. Tohoku J Exp Med 159:83–90.
Janssen U, Riley SG, Vassiliadou A, Floege J, Phillips AO. 2003. Hypertension superimposed on type II diabetes in Goto Kakizaki rats induces progressive nephropathy. Kidney Int 63:2162–2170.
Junod A, Lambert AE, Orci L, Pictet R, Gonet AE, Renold AE. 1967. Studies of the diabetogenic action of streptozotocin. Proc Soc Exp Biol Med 126:201–205.
Koulmanda M, Qipo A, Chebrolu S, O'Neil J, Auchincloss H, Smith RN. 2003. The effect of low versus high dose of streptozotocin in cynomolgus monkeys (Macaca fascilularis). Am J Transpl 3:267–272.
Kwon NS, Lee SH, Choi CS, Kho T, Lee HS. 1994. Nitric oxide generation from streptozotocin. FASEB J 8:529–533.
Lee CS, Mauer SM, Brown DM, Sutherland DE, Michael AF, Najarian JS. 1974. Renal transplantation in diabetes mellitus in rats. J Exp Med 139:793–800.
Lee HB, Seo JY, Yu MR, Uh ST, Ha H. 2007. Radical approach to diabetic nephropathy. Kidney Int 106:S67–S70.
Like AA, Rossini AA. 1976. Streptozotocin-induced pancreatic insulitis: New model of diabetes mellitus. Science 193:415–417.
Like AA, Appel MC, Williams RM, Rossini AA. 1978. Streptozotocin-induced pancreatic insulitis in mice. Morphologic and physiologic studies. Lab Invest 38:470–486.
Nagai K, Arai H, Yanagita M, Matsubara T, Kanamori H, Nakano T, Iehara N, Fukatsu A, Kita T, Doi T. 2003. Growth arrest-specific gene 6 is involved in glomerular hypertrophy in the early stage of diabetic nephropathy. J Biol Chem 278:18229–18234.
Nagasao J, Yoshioka K, Amasaki H, Tsujio M, Ogawa M, Taniguchi K, Mutoh K. 2005. Morphological changes in the rat endocrine pancreas within 12 h of intravenous streptozotocin administration. Anat Histol Embryol 34:42–47.
Nukatsuka M, Yoshimura Y, Nishida M, Kawada J. 1990. Importance of the concentration of ATP in rat pancreatic beta cells in the mechanism of streptozotocin-induced cytotoxicity. J Endocrinol 127:161–165.
Palm F. 2006. Intratenal oxygen in diabetes and a possible link to diabetic nephropathy. Clin Exp Pharm Phys 33:997–1001.
Palm F, Ortsater H, Hansell P, Liss P, Carlsson PO. 2004. Differentiating between effects of streptozotocin per se and subsequent hyperglycemia on renal function and metabolism in the streptozotocin-diabetic rat model. Diabetes Metab Res Rev 20:452–459.
Sadoff L. 1970. Nephrotoxicity of streptozotocin (NSC-85998). Cancer Chemother Rep 54:457–459.
Schein P, Kahn R, Gorden P, Wells S, Devita VT. 1973. Streptozotocin for malignant insulinomas and carcinoid tumor. Report of eight cases and review of the literature. Arch Intern Med 132:555–561.
Sotnikova R, Nosalova V, Stefek M, Stolc S, Gajdosik A, Gajdosikova A. 1999. Streptozotocin diabetes-induced changes in aorta, peripheral nerves and stomach of Wistar rats. Gen Physiol Biophys 18:155–162.
Szkudelski T. 2001. The mechanism of alloxan and streptozotocin action in B cells of the rat pancreas. Physiol Res 50:536–546.
Tay YC, Wang Y, Kairaitis L, Rangan GK, Zhang C, Harris DC. 2005. Canmurine diabetic nephropathy be separated from superimposed acute renal failure? Kindney Int 68:391–398.
Tesch GH, Nikolic-Paterson DJ. 2006. Recent insights into experimental mouse models of diabetic nephropathy. Nephron Exp Nphrol 104:e57–e62.
Tochino Y. 1987. The NOD mouse as a model of type I diabetes. Crit Rev Immunol 8:49–81.
Tojo A, Asaba K, Onozato ML. 2007. Suppressing renal NADPH oxidase to trear diabetic nephropathy. Expert Opin Ther targets 11:1011–1018.
Tomohiro T, Kumai T, Sato T, Takeba Y, Kobayashi S, Kimura K. 2007. Hypertension aggravates glomerular dysfunction with oxidative stress in a rat model of diabetic nephropathy. Life Sci 80:1364–1372.